SPECTROSCOPIC INVESTIGATION OF THE EFFECT OF POLYPHENOLIC
COMPOUNDS ON THE AMYLOID-β PROTEIN

_____

A Dissertation

Presented to

The Doctoral Program Committee

At the University of Missouri-Columbia

_____

In Partial Fulfillment

Of the Requirements for the Degree

Doctor of Philosophy

_____

By

Brittany L. Hagenhoff

Dr. Renee JiJi, Dissertation Supervisor

December 2017

The undersigned, appointed by the dean of the Graduate School,

have examined the dissertation entitled

Spectroscopic Investigation of the Effect of Polyphenolic Compounds on the Amyloid-β Protein

Presented by Brittany L. Hagenhoff,

a candidate for the degree of doctor of philosophy,

and hereby certify that, in their opinion, it is worthy of acceptance.

_____
Professor Renee D. JiJi

_____
Professor C. Michael Greenlief

_____
Professor Susan Z. Lever

_____
Professor Gary A. Weisman

ACKNOWLEDGEMENTS

TABLE OF CONTENTS

LIST OF FIGURES

LIST OF ABBREVIATIONS

AD   Alzheimer's disease

Aβ   Amyloid-β

APP   Amyloid Precursor Protein

NMR   Nuclear Magnetic Resonance

ROS   Reactive Oxygen Species

ThT   Thioflavin T

CD   Circular Dichroism

DUVRR   Deep Ultraviolet Resonance Raman

Y   Tyrosine

F   Phenylalanine

ABSTRACT

Spectroscopic Investigation of the Effect of Polyphenolic Compounds on the Amyloid-β Protein

Brittany Hagenhoff

Aggregation of the amyloid-β (Aβ) protein is associated with the development of Alzheimer's disease. Aβ is a 39-43 residue cleavage product of the amyloid precursor protein (APP). Aβ aggregates to produce insoluble plaques in the brain, which are composed of cross β-sheet structured fibrils. Various polyphenolic compounds, both naturally occurring and synthetic, have been shown to interfere with Aβ aggregation. To evaluate the ability of specific polyphenols to prevent Aβ aggregation, this investigation utilized nordihydroguaiaretic acid, curcumin, rosmarinic acid, resveratrol, piceatannol, and diethylstilbestrol. These polyphenols differ in the number of ring substituents and the atom linker between the rings. The interaction of Aβ with the polyphenolic compounds was analyzed using circular dichroism (CD) and deep ultraviolet resonance Raman (dUVRR) spectroscopies.

The polyphenols diethylstilbestrol, resveratrol, and piceatannol have increasing numbers of hydroxyl substituents on their rings, having two, three, and four respectively. It was found that with increasing number of hydroxyl ring substituents, the protein remained predominantly disordered and prevented formation of β-structure in the protein and aided in the destabilization of pre-formed Aβ fibrils. Decreasing the number of hydroxyl substituents increases the likelihood of β-sheet formation,

prevented destabilization of pre-formed Aβ fibrils, and induced loss of stability of the protein.

The polyphenols nordihydroguaiaretic acid, curcumin, and rosmarinic acid have increasing polarity respectively in the chain linker between the phenolic rings. Each of these polyphenols have four ring substituents and have four to six atoms in their chain linker. It was found that with increasing the polarity of the linker, the protein had a greater tendency to form a β-structure, however pre-formed Aβ fibrils were destabilized efficiently by all three polyphenols. Though a nonpolar chain linker pushed fibrillar protein toward a more disordered structure initially, the final state was similar regardless of added polyphenol.

Chapter I: Introduction

1.1 Alzheimer's Disease

Alzheimer's disease (AD) is a leading cause of dementia in people above the age of 65 and the sixth leading cause of death in the United States (Figure 1.1). AD is an irreversible neurodegenerative disease, and is characterized by synaptic failure, neuronal damage, and cellular degeneration in regions of the brain that mediate memory and cognitive function.[1,2,3] Diagnosis of AD is difficult as there is no single test that can diagnose the disease. AD accounts for about 60-80% of all diagnosed dementias with diagnosis made based upon clinical history, documentation of functional decline, and the ruling out of all other forms of dementia. A conformation of the diagnosis cannot be made until autopsy.[1,4]

There are two main hallmarks associated with AD which are senile plaques and neurofibrillary tangles in the plasma and cerebrospinal fluid in the brain. Plaques, which are made up of the Aβ protein, are believed to interfere with neuron communication at synapses.[1,2] Neurofibrillary tangles are made up of the tau protein and interfere with nutrient transport in neurons. [1-2,5-6]
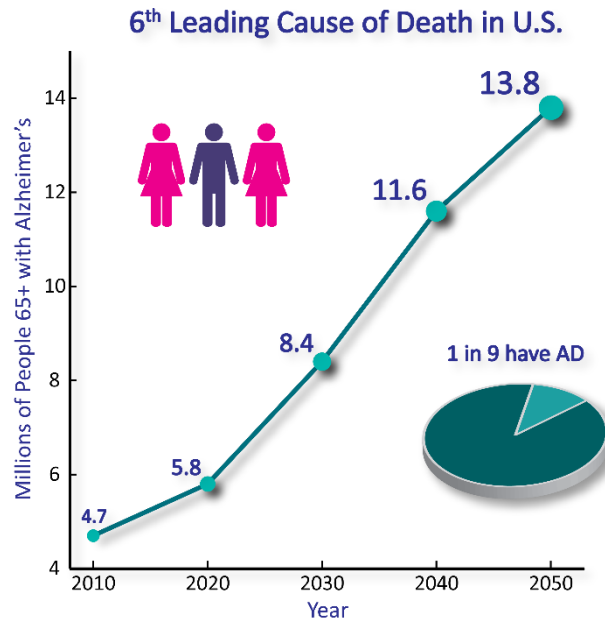
Figure 1.1: Diagnosis of Alzheimer's disease is on the rise, projected to reach nearly 14 million by year 2050. One in nine people over 65 years of age have the disease, with two out of every three of those being women.[1]

1.2 Diet and AD Prevalence

In 2010, there was an estimated 35.6 million people worldwide suffering with dementia with projections of over 65 million by 2030.[7] There are many different forms of dementia including vascular dementia, Lewy body dementia, frontotemporal dementia, normal pressure hydrocephalus dementia, and mixed dementia, all with common outward symptoms such as cognitive impairment and memory loss with about 60-80% of these diagnoses being AD.[4] The prevalence of dementia in 2010 was 2.6% in Africa, 3.9% in Asia, 6.2% in Europe, and 6.5% in the Americas. [7] Many ethnic groups living in the United States have much higher AD prevalence rates than those living in their homelands.[7] Studies of these populations show that 6.24 % of Nigerians living in the United States suffered from AD whereas only 1.41% of Nigerians suffered in Ibadan,

Nigeria. In the United States, 4.1% Japanese suffered from AD, while AD prevalence in Japan was only 1.88%.[8-10]

The prevalence of AD among different ethnicities in the United States is roughly ranked as African Americans and Hispanics > American and European whites > Asian Americans > Native Americans.[1,7,11] One of the primary differences among these ethnic groups is that they vary in location. A potentially unifying factor that could influence the chance of developing AD may be location and more specifically, diet. Different ethnicities and cultures have different eating and drinking habits, which could very well be one of the factors at the root of the differences in AD prevalence.

As one would assume, eating healthy should keep your overall health in good standing. The food pyramid is one representation of a healthy diet. However, which foods comprise the food pyramid varies depending on region. In general, high consumption of meat, butter, high-fat dairy products, eggs, refined sugar, saturated fatty acids, high caloric intake, and excessive alcohol consumption has a negative association with brain health, whereas diets rich in fruits, vegetables, fish, tea, coffee, and whole grains has a positive association.[12-13] A diet that follows this general trend of high fresh food intake and low meat and fat intake is the Mediterranean diet. The Mediterranean diet consists of:[13-17]

- High intake of vegetables, legumes, fruits, nuts and seeds, potatoes, breads and cereals, and olive oil

- Moderate intake of fish

- Low to moderate intake of dairy products (cheese and yogurt) from goat, sheep, buffalo, cow and camel

- Low intake of meat and poultry

- Low to moderate amount of alcohol wine

- Condiments, i.e., garlic, onion, and herbs

- Desserts of fresh fruit or sweets containing concentrated sugars or honey

Olive oil is the main source of fat, unlike in Western diets where animal fats are more common. Also, Western diets are higher in dairy products. [14-16] The traditional Japanese diet is similar to the Mediterranean diet in that it is made up of mainly fish and plant foods, and is limited in animal fats.[31] Conversely, the Western diet is comprised mostly of red and processed meats, refined grains, sweets, and moderate alcohol intake.[15,17] These differences could be the reason that AD prevalence is higher in the U.S and Northern Europe than in the Mediterranean region and Japan.

Adherence to a healthy diet, much like the Mediterranean diet has been associated with reduced risk of cardiovascular disease and cancers, lowered rates of chronic diseases, reduced risk of neurodegenerative disease, reduced risk of AD, better cognitive functioning, and overall longer life expectancy.[13,18-21]

1.3 Amyloid-β

The buildup of the Aβ protein into plaques is a hallmark of AD.[1] Aβ is a ~4 kDa protein that is 39-43 residues long. It is produced from the proteolytic cleavage of the transmembrane amyloid precursor protein (APP) by β-secretase and γ-secretase.[22-24]

Once Aβ is cleaved from APP, the monomer can self-aggregate into various sized oligomers.[25-27] The oligomers are transient in nature, changing size and structure quickly, making individual species difficult to isolate. The suggested mechanism in which the aggregation occurs (Figure 1.2) can differ for each oligomeric species as well. Unsystematic intermediates can form between monomers and oligomers before forming a fibril.[25-26, 28-29]

One type of intermediate that can form is the protofibril. Protofibrils are short, flexible fibrils which are precursors of longer, more rigid fibrils.[28-29] The occurrence of protofibrils decreases as fibril formation increases.[29] The process of fibril formation by protofibril aggregation into mature fibrils is irreversible; they do not dissociate into protofibrils.[29] All forms of Aβ from monomers to high molecular weight oligomers have proven to be neurotoxic.[23]
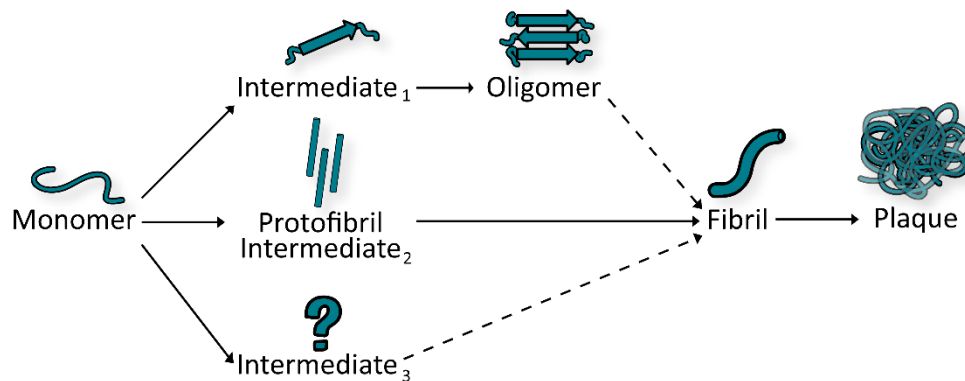
Figure 1.2: Proposed aggregation mechanism of Aβ.

The different species present in the aggregation pathway can take on different types of protein secondary structure. The Aβ monomer is disordered in structure and as the protein begins to aggregate, it becomes more ordered forming β-sheet secondary structure.[25-26,28-29] These secondary structures are based on the dihedral angles around

C_α of an amino acid in the protein backbone, phi and psi.[30] The disordered secondary structure means there is no order, or more specifically, no one set of dihedral angles. The β-sheet secondary structure can be categorized into two types; parallel and anti-parallel. Parallel β-strands align themselves in the same direction with carbonyl and amide groups staggered. Anti-parallel β-strands align themselves in opposite directions with carbonyl and amide groups lining up. Parallel β-sheets have phi and psi angles of 119° and 113°, respectively, and anti-parallel β-sheets have phi and psi angles of -139° and 135^0, respectively.[31]

1.4 Polyphenols

1.4.1 Polyphenols and Aβ

Polyphenols have been shown to reduce the toxicity of various forms of Aβ and play a role in the Aβ aggregation process.[32] Structurally, polyphenols are aromatic rings with hydroxyl group substituents that are naturally found in plants and foods with over 8,000 compounds identified.[32-33]

As previously mentioned, Aβ can self-aggregate in various ways and into various sized oligomers, changing in size and structure quickly.[25-29] Although the exact mechanism is unknown, a general classification of polyphenols based on how they act on the aggregation of Aβ can be made. The three classifications are those that prevent the formation of fibrils, those that prevent the extension of fibrils, and those that can destabilize pre-formed fibrils.[33,35]

1.4.2 Structural Differences (Hydrophobicity vs Antioxidant Potency)

Polyphenols vary widely in structure. They can be sub-classified into many groups based on structure, such as flavonoids, stilbenes, or lignans. The flavonoid group is the largest polyphenol group, with over 6,000 flavonoids identified, and has sparked research in many areas.[32-33,36] All flavonoids have a similar (C_6-C_3-C_6) structure with two aromatic rings bound by a 3-carbon formed oxygenated heterocycle which makes up a third ring, and differ mainly in the substituents on the rings.[37] Stilbenes have a similar structure to flavonoids except for one less carbon that prevents the third ring from forming (i.e., C_6-C_2-C_6). Instead, the two rings are connected by a double bond; i.e., methylene bridge.[32,37] Lignans are a combination of two phenylpropane units where two C_6-C_3 structures are attached at their central (C_8) carbon.[32-33,38] Some polyphenols do not fall into a specific classification and are grouped as an "other polyphenol".

Flavonoids have been heavily researched due to their vast abundance. However, the focus of this research is on non-flavonoid polyphenols such as stilbenes and other polyphenols. Depending on the classification of the polyphenol, different structural characteristics are present. In this investigation, the polyphenols used were each linear polyphenols (non-flavonoid) each with two rings, a chain linker between the rings, and hydroxyl group substituents on the rings.

Polyphenols can act upon any stage of the Aβ aggregation process, with certain structural characteristics suiting early or late stages more appropriately. Recent studies have surfaced that deal with the structural significance of polyphenols. [34,38-39] Certain

characteristics that can play a role on how it will behave are the number and type of substituents on the rings, length of the atom linker between the rings, and the polarity of the atom linker. An example of a generic polyphenol is shown in Figure 1.3.
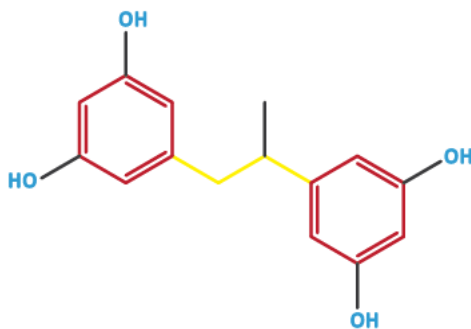
Figure 1.3: Generic polyphenol model: hydroxyl group substituents (blue), aromatic rings (red), and an atom linker chain (yellow).

1.4.3 Polyphenol Structural Characteristics

Hydrophobicity and antioxidant potency of polyphenols have been shown to affect their ability to inhibit Aβ aggregation. It is believed that hydrophobicity interferes with the formation and extension stages, whereas antioxidative potency affects the fibrillization stages.[34]   Two rings with a minimum of two to three hydroxyl substitutions on those rings is preferred.[34]   Polyphenols can interact with proteins through a multitude of ways, including aromatic π-π stacking interactions between the polyphenolic rings and aromatic residues, hydrogen bonding between the hydroxyl substituents and the protein backbone, and hydrophobic interactions.[34,40-45]

Structurally, a polyphenol with both high hydrophobicity and antioxidant potency would be the most desirable for preventing Aβ aggregation. This would allow binding to hydrophobic motifs of the protein, interference with aromatic stacking that could facilitate aggregation, formation of hydrogen bond which could weaken salt bridges between aggregating Aβ species, and provide free radical scavenging.[34]

Binding of each individual polyphenol to the Aβ protein not only depends on the polyphenol's structure but also which Aβ species it is binding to along the aggregation pathway. Disordered monomers versus small oligomers versus β-sheet fibrils will bind polyphenols by different means due to their variation of secondary and higher order structure. Typically, polyphenols interact with the peptide at residues such as tyrosine-10 and phenylalanines-4, 19, and 20 due to π-stacking interactions of the aromatic residues with the phenolic rings of the polyphenol.[46-47]

Isolated segments of the protein change in secondary structure differently. For example, the C-terminus has a higher probability of rapid oligomerization due to the increased number of nonpolar residues.[46] Lührs et al. showed two parallel β-sheets that run along the fibril axis from residues ≈18-26 and ≈31-42 through the use of hydrogen/deuterium-exchange nuclear magnetic resonance (NMR) spectroscopy.[48] Polyphenols interacting with residues within this region could prevent the β-strands from developing. Polyphenols such as curcumin have been shown to interact with residues in this region including phenylalanines-19 and 20, serine-26, isoleucine-32, and methionine-35 as well as within the loop of these β-strands at lysine-28.[47-48] Once β-strands have formed, polyphenols such as rosmarinic acid and resveratrol, have been shown to hydrogen bond along the side of β-sheet amyloid structures promoting destabilization of fibrils.[47,49]

1.5   Polyphenols and Oxidation

Polyphenols are famous for their antioxidative properties and are abundant in fruits, vegetables, and beverages, such as tea and red wine. Free radicals are products

of naturally occurring processes in cells, which in turn cause oxidative stress in the cells that can lead to cell death. Antioxidants remove free radicals by scavenging them.[50] Polyphenols have been known to possess hepatoxic, antioxidant, anti-inflammatory, antimicrobial, anticancer, antiviral, anti-allergic, and anti-ulcer effects.[33] Polyphenols have many different biological actions, such as interaction with transition metals, inactivation of free radicals, precipitation of protein, inhibition of inflammatory response, modulation of the activity of different enzymes, and effects on intracellular signaling pathways and gene expression.[51-54]

Reactive oxygen species (ROS) are free radicals with a single unpaired electron that are produced during naturally occurring cellular processes that can damage proteins, nucleic acids, and lipid membranes leading to membrane instability eventually causing apoptosis. [55-56] Oxidative stress occurs when the generation of ROS is higher than the level of antioxidants acting against them. Examples of ROS are superoxide anions (O_2^{-}), hydroxyl radicals ($OH^{.}$), and hydrogen peroxide (H_2O_2).[57] Increasing polyphenol intake can combat ROS generation due to the ability of polyphenols to donate a hydrogen atom to lipids and other molecules, thereby preventing their oxidation by ROS.[54]

Protein oxidation and increased oxidative stress has been shown in numerous studies to lead to the manifestations of AD.[57-58] The brain is particularly susceptible to free radical damage due to a high content of easily peroxidizable lipids, a high rate of oxygen consumption, and a lack of antioxidants in relation to other organs in the body.[2,58-59] Protein oxidation impairs protein synthesis, neuronal function, enzyme

activation, and the ability of cells to regulate homeostasis leading to cognitive decline.[59-60]

ROS produce oxidative stress which induces intracellular Aβ accumulation in cell cultures and Aβ itself has been shown to induce oxidative stress in vivo and in vitro.[36,62-66] Studies have shown that lipid peroxidation is enhanced by increases in intracellular Aβ.[63] The oxidation of the methionine-35 residue in Aβ could play an important role in free radical and oxidative stress generation.[2,63,65] The tyrosine-10 residue is also an easy target of oxidation in the protein.[2,63] Studies by Murakami et al. have shown that the oxidation of tyrosine-10 could be lead to oxidation of the methionine-35 residue, thereby contributing to the increase in free radical concentration and neurotoxicity of the protein.[63] Thus, a vicious cycle between ROS and Aβ accumulation may accelerate the progression of AD.

1.6 Spectroscopic Techniques Used

Spectroscopic techniques are frequently utilized for analysis of biological samples, such as proteins. Different forms of spectroscopy instrumentation were implemented throughout this study. For Aβ, Thioflavin T (ThT) assays are commonly used to monitor fibril formation. In order to observe the secondary structure, two different forms of spectroscopy are commonly used, circular dichroism (CD) and deep ultraviolet resonance Raman (dUVRR).

The ThT assay is a fluorescence based method that can monitor the formation of Aβ fibrils in solution over time. The fluorophore selectively binds to β-sheet fibrils

(Figure 1.4) causing it to fluoresce.[67] The assay confirms the presence of cross-β-sheet

structure, which is only present in amyloid fibrils.
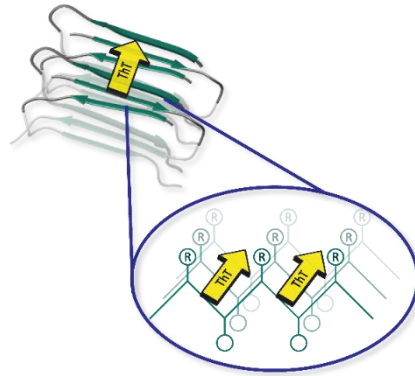
Figure 1.4: ThT binds in the grooves of β-sheet fibrils increasing fluorescence.

CD involves illuminating samples with circularly polarized light and then

measuring the difference in absorption of left and right polarized light.[68] Depending on

the secondary structure of the protein and the dihedral angles that correspond with the

structure, the light will be absorbed differently producing characteristic CD spectra as

seen in Figure 1.5. If the protein is lacking defined structure and is disordered, a strong

minimum at 197 nm and a slight maximum at 217 nm will be observed. For a β-sheet

structured protein, the spectrum is nearly flipped with a strong minimum at 217 nm and

a slight maximum at 197 nm. From this, classification of secondary structure was

obtained as well as the changes in the structure over time.
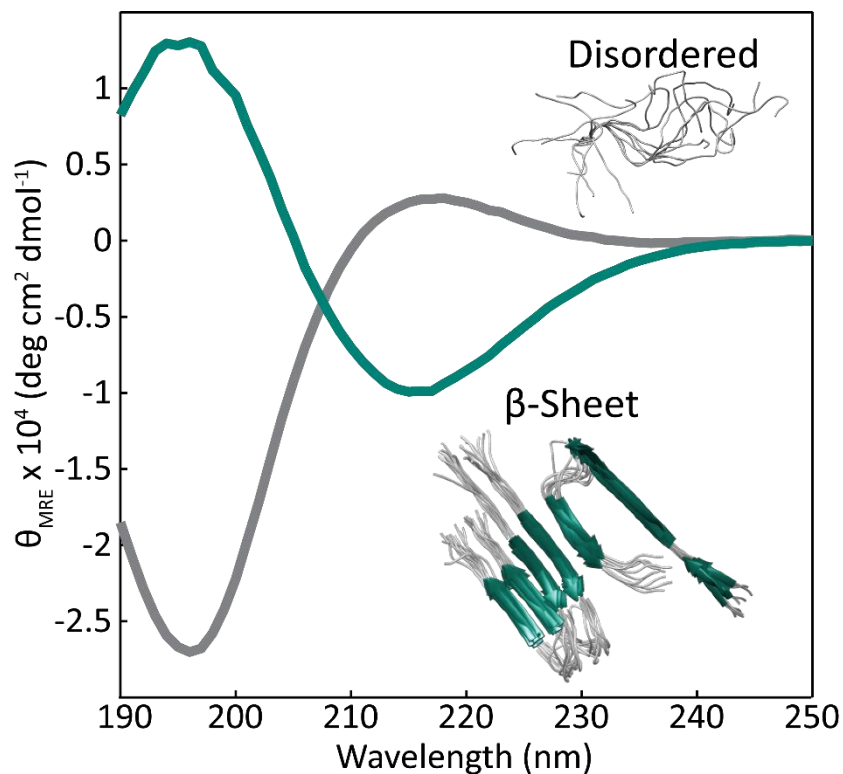
Figure 1.5: CD spectra of secondary structure seen in Aβ aggregation; disordered structure (grey) with a negative minimum at 197 nm and a slight positive maximum at 217 nm, and β-sheet (teal) with a positive minimum at 197 nm and a negative minimum at 217 nm.

DUVRR is an emerging technique for the determination of secondary structure changes of a protein. Raman is an inelastic scattering method in which the emitted light from molecules is shifted to different frequencies than the incident excitation light.[69] With dUVRR, the laser excites within the deep UV region and enhances the vibrational modes of the amide backbone, as well as aromatic side chains.[70] DUVRR spectra of proteins have four protein backbone associated amide bonds; amide I (C=O stretching) at 1650-1680 cm^{-1}, amide II (C-H/N-H in phase stretching/bending) at 1480-1560 cm^{-1}, amide III (C-H/N-H out of phase stretching/bending) at 1240-1315cm^{-1}, and amide S (coupled C-H/N-H bending) at 1350-1400 cm^{-1}, as seen in Figure 1.6.[71] Intensity changes in these regions signify changes in secondary structure. When a protein

changes from disordered to β-sheet, there are not typically high intensity changes in the amide modes. There can be shift in the amide S mode when transitioning between these two structures as well as slight intensity changes in amide I. There can also be changes in the environment of the aromatic residues of the protein. Aβ contains tyrosine (Y) and phenylalanine (F). The Y1 tyrosine modes are at 820 and 858 cm^{-1} and the Y9a, Y7a, and Y8b tyrosine modes are present at 1191, 1213, and 1608 cm^{-1}, respectively.[72] The phenylalanine modes are represented by the F12 mode at 1008 cm^{-1}, F mode at 1191 and 1213 cm^{-1}, and F8b and F8a modes at 1586 and 1608 cm^{-1}, respectively.[72] With the use of these different spectroscopic techniques, the impact of polyphenols on the aggregation of Aβ can be determined.
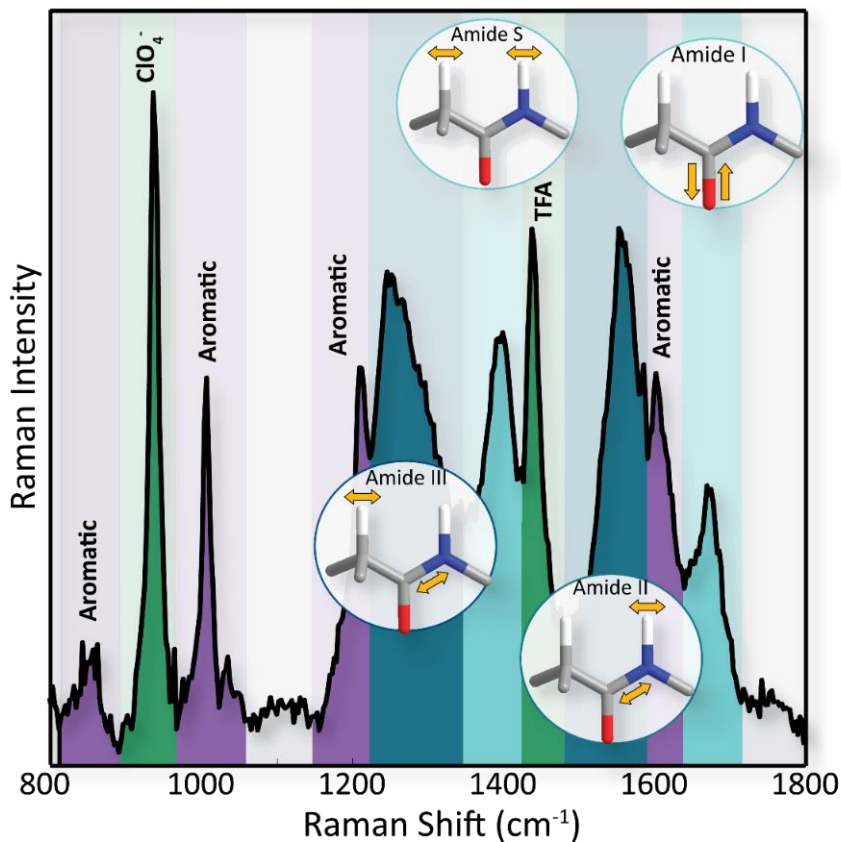
Figure 1.6: Amide and aromatic modes present in a protein dUVRR spectrum.

1.7 References

1.   Alzheimer's ssocation. 2014 Alzheimer's disease facts and figures. *Alzheimer's & Dementia* **2014,** *10* (2), 4-28.

2.   Masters, C. L.; Cappai, R.; Barnham, K. J.; Villemagne, V. L., Molecular mechanisms for Alzheimer's disease: implications for neuroimaging and therapeutics. *J Neurochem* **2006,** *97* (6), 1700-25.

3.   Pike, C. J. B., D.; Walencewicz, A. J.; Glabe, C. G.; Cotman, C. W., Neurodegeneration Induced by β-Amyloid peptides in vitro: the role of peptide assembly state. *J Neurosci* **1993,** *13* (4), 1676-1687.

4.   Neugroschl, J.; Wang, S. Alzheimer's disease: Diagnosis and treatment across the spectrum of disease severity. *Mt Sinai J Med* **2012,** *78* (4), 596-612.

5.   Alzheimer's Disease. http://nihseniorhealth.gov/alzheimersdisease/whatisalzheimersdisease/01.html.

6.   Haass, C. S., M. G.; Hung, A. Y.; Vigo-Pelfrey, C.; Mellon, A.; Ostaszewski, B. L.; Lieberburg, I.; Koo, E. H.; Schenk, D.; Teplow, D. B.; Selkoe, D. J. , Amyloid-beta peptide is produced by cultured cells during normal metabolism. *Nature* **1992,** *359*, 322-325.

7.   World Alzheimer Report - Executive Summary. *Alzheimer's Disease* **2009**, 6-8.

8.   White, L.; Petrovitch, H.; Ross, G. W.; Masaki, K. H.; Abbott, R. D.; Teng, E. L.; Rodriguez, B. L.; Blanchette, P. L.; Havlik, R. J.; Wergowske, G.; Chiu, D.; Foley, D. J.; Murdaugh, C.; Curb, D., Prevalence of dementia in older Japanese-American men in Hawaii. *JAMA* **1996,** *276* (12), 955-960.

9.   Hendrie, H. C.; Osuntokun, B. O.; Hall, K. S., Prevalence of Alzheimer's disease and dementia in two communities: Nigerian Africans and African Americans. *Am J Psychiatry* **1995,** *152* (10), 1485-1492.

10. Graves, A. B.; Larson, E. B.; Edland, S. D.; Bowen, J. D.; McCormick, W. C.; McCurry, S. M.; Rice, M. M.; Wenzlow, A.; Uomoto, J. M., Prevalence of dementia and its subtypes in the Japanese American population of King County, Washington State. *Am J Epidemiol* **1996,** *144* (8), 760-771.

11. Mehta, K. M.; Yeo, G. W., Systematic review of dementia prevalence and incidence in US race/ethnic populations. *Alzheimers Dement* **2017,** *13,* 72-83.

12. Morris, M. C.; Evans, D. A.; Bienias, J. L.; Tangney, C. C.; Bennett, D. A.; Wilson, R. S.; Aggarwal, N.; Schneider, J., Consumption of fish and n-3 fatty acids and risk of incident Alzheimer disease. *Arch Neurol* **2003,** *60,* 940-946.

13. Hu, N.; Yu, J. T.; Tan, L.; Wang, Y. L.; Sun, L.; Tan, L., Nutrition and the risk of Alzheimer's disease. *Biomed Res Int* **2013,** *2013,* 1155-1167.

14. Gillette-Guyonnet, S.; Vellas, B., Diet and prevention of cognitive decline and dementia. *Canadian Review of Alzheimer's Disease and Other Dementias* **2007,** *September, 18*-27.

15. Willet, W. C.; Sacks, F.; Trichopoulou, A.; Drescher, G.; Perro-Luzzi, A.; Helsing, E.; Trichopoulou, D., Mediterranean diet pyramid: a cultural model for healthy eating. *Am J Clin Nutr* **1995,** *61,* 1402S-1406S.

16. Kromhout, D.; Keys, A.; Aravanis, C.; Buzina, R.; Fidanza, F.; Giampaoli, S.; Jansen, A.; Menotti, A.; Ndeljkovic, S.; Pekkarinen, M.; Simic, B. S.; Toshima, H., Food consumption patterns in the 1960s in seven countries. *Am J Clin Nutr* **1989,** *49,* 889-894.

17. Allbaugh, L. G., Crete: a case study of an underdeveloped area. Princeton University Press: Princeton, NJ, 1953.

18. Kesse-Guyot, E.; Andreeva, V. A.; Jeandel, C.; Ferry, M.; Hercberg, S.; Galan, P., A healthy dietary pattern at midlife is associated with subsequent cognitive performance. *J Nutr* **2012,** *142* (5), 909-915.

19. Hankey, G. J., Nutrition and the risk of stroke. *The Lancet Neurology* **2012,** *11* (1), 66-81.

20. Feart, C. S., C.; Rondeau, V.; Amieva, H.; Portet, F.; Dartigues, JF.; Scarmeas, N.; Barberger-Gateau, P., Adherence to a Mediterranean diet, cognitive decline, and risk of dementia. *JAMA* **2009,** *302* (6), 638-648.

21.   Willet, W. C., Diet and Health: What Should We Eat? *Science* **1994,** *264*, 532-537.

22.   Kang, J.; Lemaire, H. G.; Unterbeck, A.; Salbaum, J. M.; Masters, C. L.; Grzeschik, K. H.; Multhaup, G.; Beyreuther, K.; Muller-Hill, B., The precursor of Alzheimer's disease amyloid A4 protein resembles a cell-surface receptor. *Nature* **1987,** *325* (6106), 733-736.

23.   Cappai, R. W., A. R. , Amyloid β. *Int Biochem & Cell Bio* **1999,** *31* (9), 885-889.

24.   Glenner, G. G.; Wong, C. W., Alzheimer's disease: initial report of the purificaiton and characterization of a novel cerebrovascular amyloid protein. *Biochem Biophys Res Commun* **1984,** *16* (120), 885-890.

25.   Ono, K.; Li, L.; Takamura, Y.; Yoshiike, Y.; Zhu, L.; Han, F.; Mao, X.; Ikeda, T.; Takasaki, J.; Nishijo, H.; Takashima, A.; Teplow, D. B.; Zagorski, M. G.; Yamada, M., Phenolic compounds prevent amyloid beta-protein oligomerization and synaptic dysfunction by site-specific binding. *J Biol Chem* **2012,** *287* (18), 14631-43.

26.   Necula, M.; Kayed, R.; Milton, S.; Glabe, C. G., Small molecule inhibitors of aggregation indicate that amyloid beta oligomerization and fibrillization pathways are independent and distinct. *J Biol Chem* **2007,** *282* (14), 10311-10324.

27.   Roychaudhuri, R.; Yang, M.; Deshpande, A.; Cole, G. M.; Frautschy, S.; Lomakin, A.; Benedek, G. B.; Teplow, D. B., C-terminal turn stability determines assembly differences between Abeta40 and Abeta42. *J Mol Biol* **2013,** *425* (2), 292-308.

28.   Walsh, D. M.; Lomakin, A.; Benedek, G. B.; Condron, M. M.; Teplow, D. B., Amyloid B-Protein Fibrillogenesis. *J Biol Chem* **1997,** *272*, 22364-22372.

29.   Harper, J. D.; Wong, S. S.; Lieber, C. M.; Lansbury, P. T., Observation of metastable AB amyloid protofibrils by atomic force microscopy. *Chem Biol* **1997,** *4*, 119-125.

30.   Ramachandran, G. N.; Ramakrishnan, C.; Sasisekharan, V. Stereochemistry of polypeptide chain configurations. *J Mol Biol* **1963,** *7*, 95-99.

31.   Pauling, L.; Corey, R. B., The pleated sheet, a new layer configuration of polypeptide chains. *Proc Natl Acad Sci* **1951,** *37,* 251-256.

32.   Lakey-Beitia, J.; Berrocal, R.; Rao, K. S.; Durant, A. A., Polyphenols as therapeutic molecules in Alzheimer's disease through modulating amyloid pathways. *Mol Neurobiol* **2015,** *51* (2), 466-479.

33.   Odeh, F.; Al-Jaber, H.; Khater, D., Nanoflora — How nanotechnology enhanced the use of active phytochemicals. *Application of Nanotechnology in Drug Delivery* **2014,** *Chapter 10*, 344-346.

34.   Shoval, H.; Lichtenberg, D.; Gazit, E., The molecular mechanisms of the anti-amyloid effects of phenols. *Amyloid* **2007,** *14* (1), 73-87.

35.   Ono, K.; Yoshiike, Y.; Takashima, A.; Hasegawa, K.; Naiki, H.; Yamada, M., Potent anti-amyloidogenic and fibril-destabilizing effects of polyphenols in vitro: implications for the prevention and therapeutics of Alzheimer's disease. *J Neurochem* **2003,** *87* (1), 172-181.

36.   Harnly, J. M.; Doherty, R. F.; Beecher, G. R.; Holden, J. M.; Haytowitz, D. B.; Bhagwat, S.; Gebhardt, S., Flavonoid content of U.S. fruits, vegetables, and nuts. *J Agric Food Chem* **2006,** *54*, 9966-9977.

37.   Li, F. G., Q.; Dong, H.; Shi, J., Resveratrol, a neuroprotective supplement for Alzheimer's disease. *Curr Pharm Des* **2012,** *18*, 27-33.

38.   Manach, C. S., A.; Morand, C.; Remesy, C.; Jimenez, L., Polyphenols: food sources and bioavailability. *Am J Clin Nutr* **2004,** *79*, 727-747.

39.   Churches, Q. I.; Caine, J.; Cavanagh, K.; Epa, V. C.; Waddington, L.; Tranberg, C. E.; Meyer, A. G.; Varghese, J. N.; Streltsov, V.; Duggan, P. J., Naturally occurring polyphenolic inhibitors of amyloid beta aggregation. *Bioorg Med Chem Lett* **2014,** *24* (14), 3108-3112.

40.   Porat, Y.; Abramowitz, A.; Gazit, E., Inhibition of amyloid fibril formation by polyphenols: structural similarity and aromatic interactions as a common inhibition mechanism. *Chem Biol Drug Des* **2006,** *67* (1), 27-37.

41.   Gazit, E., Mechanisms of amyloid fibril self-assembly and inhibition: Model short peptides as a key research tool. *FEBS J* **2005,** *272*, 5971-5978.

42.   Gazit, E., Global analysis of tandem aromatic octapeptide repeats: The significance of the aromatic-glycine motif. *Bioinformatics* **2002,** *18* (6), 880-883.

43.   Porat, Y.; Mazor, Y.; Efrat, S.; Gazit, E., Inhibition of islet amyloid polypeptide fibril formation: a

        potential role for heteroaromatic interactions. *Biochemistry* **2004,** *43*, 14454-14462.

44.   Azriel, R.; Gazit, E., Analysis of the minimuml amyloid-forming fragment of the islet amyloid

        polypeptide. An experimental support for the key role of the phenylalanine residue in amyloid

        formation. *J Biol Chem* **2001,** *276* (36), 34156-34161.

45.   Hudson, S. A.; Ecroyd, H.; Dehle, F. C.; Musgrave, I. F.; Carver, J. A., (-)-Epigallocatechin-3-gallate

        (EGCG) maintains kappa-casein in its pre-fibrillar state without redirecting its aggregation

        pathway. *J Mol Biol* **2009,** *392* (3), 689-700.

46.   Serpell, L. C. Alzheimer's amyloid fibrils: structure and assembly. *BBA - Mol Basis Dis* **2000,** *1502*

        (1), 16-30.

47.   Wang, Y.; Latshaw, D. C.; Hall, C. K. Aggregation of Aβ(17-36) in the presence of naturally

        occuring phenolic inhibitiors using coarse-grained simulations. *J Mol Bio* **2017,** *In-press.* [Online

        early access]. http://www.sciencedirect.com/science/article/pii/S0022283617304886.

48.   Lührs, T.; Ritter, C.; Adrian, M.; Riek-Loher, D.; Bohrmann, B.; Döbeli, H.; Schubert, D.; Riek, R. 3D

        structure of Alzheimer's amyloid-β (1-42) fibrils. *PNAS* **2005,** *102* (48), 17342-17347.

49.   Ramazzotti, M.; Melani, F.; Marchi, L.; Mulinacci, N.; Gestri, S.; Tiribilli, B.; Degl'Innocenti, D.

        Mechanisms for the inhibition of amyliod aggregation by small ligands. *Biosci Rep* **2016,** *36* (5), 1-

        14.

50.   Choi, D. Y.; Lee, Y. J.; Hong, J. T.; Lee, H. J., Antioxidant properties of natural polyphenols and

        their therapeutic potentials for Alzheimer's disease. *Brain Res Bull* **2012,** *87* (2-3), 144-153.

51.   Obrenovich, M. E.; Nair, N. G.; Beyaz, A.; Aliev, G.; Reddy, V. P., The role of polyphenolic

        antioxidants in health, disease, and aging. *Rejuvention Res* **2010,** *13* (6), 631-643.

52.   Rojanathammanee, L.; Puig, K. L.; Combs, C. K., Pomegranate polyphenols and extract inhibit

        nuclear factor of activated T-cell activity and microglial activation in vitro and in a transgenic

        mouse model of Alzheimer disease. *J Nutr* **2013,** *143* (5), 597-605.

53.   Bravo, L., Polyphenols: chemistry, dietary sources, metabolism, and nutritional significance.

        Nutritions Reviews **1998,** *56* (11), 317-333.

54.   Sun, A. Y.; Wang, Q.; Simonyi, A.; Sun, G. Y., Botanical phenolics and brain health. *Neuromolecular Med* **2008,** *10* (4), 259-274.

55.   Romano, A. D.; Serviddio, G.; de Matthaeis, A.; Bellanti, F.; Vendemiale, G., Oxidative stress and aging. *J Nephrol* **2010,** *23* (S15), S29-S36.

56.   Nunomura, A.; Castellani, R. J.; Zhu, X.; Moreira, P. I.; Perry, G.; Smith, M. A., Involvement of oxidative stress in Alzheimer disease. *J Neuropathol Exp Neurol* **2006,** *65* (7), 631-641.

57.   Keller, J. N.; Schmitt, F. A.; Scheff, S. W.; Ding, Q.; Chen, Q.; Butterfield, D. A.; Markesbery, W. R., Evidence of increased oxidative damage in subjects with mild cognitive impairment. *Neurology* **2005,** *64*, 1152-1156.

58.   Floyd, R. A.; Hensley, K., Oxidative stress in brain aging - Implications for therapeutics of neurodegenerative diseases. *Neurobio Aging* **2002,** *23*, 795-807.

59.   Mattson, M. P.; Chan, S. L.; Duan, W., Modification of brain aging and neurodegenerative disorders by genes, diet, and behavior. *Physiol Rev* **2002,** *82*, 637-672.

60.   Ding, Q.; Markesbery, W. R.; Chen, Q.; Li, F.; Keller, J. N., Ribosome dysfunction is an early event in Alzheimer's disease. *J Neurosci* **2005,** *25* (40), 9171-9175.

61.   Berlett, B. S.; Stadtman, E. R. Protein oxidation in aging, disease, and oxidative stress. *J Bio Chem* **1997,** *272,* 20313-20316.

62.   Rinaldi, P.; Polidori, M. C.; Metastasio, A.; Mariani, E.; Mattioli, P.; Cherubini, A.; Catani, M.; Cecchetti, R.; Senin, U.; Mecocci, P., Plasma antioxidants are similarly depleted in mild cognitive impairment and in Alzheimer's disease. *Neurobiology of Aging* **2003,** *24* (7), 915-919.

63.   Misonou, H.; Marishima-Kawashima, M.; Ihara, Y., Oxidative stress induces intracellular accumulation of Amyloid β-protein (Aβ) in human neuroblastoma cells. *Biochemistry* **2000,** *39*, 6951-6959.

64.   Paola, D.; Domenicotti, C.; Nitti, M.; Vitali, A.; Borghi, R.; Cottalasso, D.; Zaccheo, D.; Odetti, P.; Strocchi, P.; Marinari, U. M.; Tabaton, M.; Pronzato, M. A., Oxidative stress induces increase in intracellular amyloid beta-protein production and selective activation of betaI and betaII PKCs in NT2 cells. *Biochem Biophys Res Commun* **2000,** *268* (2), 642-646.

65. Murakami, K.; Irie, K.; Ohigashi, H.; Hara, H.; Nagao, M.; Shimizu, T.; Shirasawa, T., Formation and stabilization model of the 42-mer Aβ radical - Implications for the long-lasting oxidative stress in Alzheimer's disease. *J Am Chem Soc* **2005,** *127*, 15168-15174.

66. Tabner, B. J.; El-Agnaf, O. M.; Turnbull, S.; German, M. J.; Paleologou, K. E.; Hayashi, Y.; Cooper, L. J.; Fullwood, N. J.; Allsop, D., Hydrogen peroxide is generated during the very early stages of aggregation of the amyloid peptides implicated in Alzheimer disease and familial British dementia. *J Biol Chem* **2005,** *280* (43), 35789-35792.

67. Schoneich, C., Methionine oxidation by reactive oxygen species: reaction mechanisms and relevance to Alzheimer's disease. *Biochim Biophys Acta* **2005,** *1703* (2), 111-119.

68. Coalier, K. A.; Paranjape, G. S.; Karki, S.; Nichols, M. R. Stability of early-stage amyloid-β (1-42) aggregation species. *BBA* **2013,** *1834,* 65-70.

69. Greenfield, N. J. Analysis of circular dichroism data. *Methods in Enzymology* **2004,** *383,* 282-317.

70. Mikhonin, A. V. Direct UV resonance Raman monitoring of protein folding reaction coordinate: alpha-helix melting and formation revisited. Ph. D Thesis, University of Pittsburgh, **2006.**

71. Wang, Y.; Purrello, R.; Jordan, T.; Spiro, T. G. UVRR spectroscopy of the peptide bond. 1. Amide S, a nonhelical structure marker, is a C$_\alpha$H bending mode. *J Am Chem Soc* **1991,** *113,* 6359-6368.

72. Austin, J. C.; Jordan, T.; Spiro, T. G. Ultraviolet resonance Raman studies of proteins and related model compounds. Chapter 2. *Biomolecular Spectroscopy, Part A*. Clark, R. J. H.; Hester, R. E. John Wiley & Sons Ltd. **1993**; 55-127.

Chapter II: Increasing Ring Substituents Decreases β-sheet Formation

2.1 Abstract

Stilbenoids have common structural components consisting of two phenolic rings with hydroxyl group substituents and a chain linker between the rings. Hydroxyl group substituents on the polyphenolic rings not only facilitate hydrogen bonding with the protein backbone but also provide antioxidant properties. The antioxidant capacity increases with the number of substituents. This study investigated the ability of stilbenoids, differing in the number of hydroxyl substituents to prevent β-sheet fibril formation. The polyphenols diethylstilbestrol, resveratrol, and piceatannol are structurally similar, differing in the number of hydroxyl group substituents, having two, three, and four, respectively. It was found that with increasing number of hydroxyl ring substituents on the polyphenols, the protein remained more disordered and formed smaller amounts of β-structure. Diethylstilbestrol, with only two ring substituents, did not prevent formation of β-sheet structure, which could in turn lead to the formation of fibrillar plaques in the brain.

2.2 Introduction

Hydroxyl group substituents on polyphenolic rings allow for essential binding to the proteins through hydrogen bonding of the polyphenol to the amide rich backbone of the proteins.[1-3] Studies have shown that greater numbers of hydroxyl groups on polyphenols, is correlated with higher the antioxidant activity.[4] Ono et al. compared four flavonoid compounds (myricetin, morin, quercetin, and kaempferol) that have similar structures and differ only in the numbers of hydroxyl substituents. It was found that decreasing the number of hydroxyl substituents decreased the anti-amyloidogenic and fibril-destabilizing activity of the polyphenol.[4]

This study sought to determine the effect of the number of hydroxyl substituents on stilbenoids compounds, on their ability to prevent β-sheet fibril formation. The polyphenols diethylstilbestrol, resveratrol, and piceatannol have two, three, and four hydroxyl substituents on their rings, respectively. They each have a 2-atom carbon chain between the two rings allowing for a conjugated double bond system in the molecule.

Piceatannol is a naturally occurring stilbenoids found in plants such as Japanese knotweed, as well as in fruits including many grape families. [5] Figure 2.1 shows the structure of the first polyphenol analyzed, piceatannol.
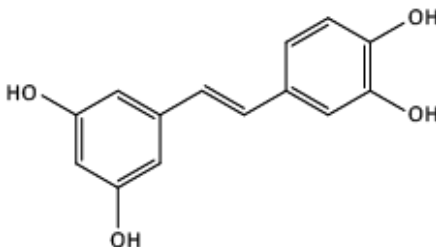
Figure 2.1: Structure of piceatannol.

Resveratrol is found in many fruits, such as grapes, blueberries, and cranberries, and is famous for its presence in red wines.[6] Resveratrol, shown in Figure 2.2, has one less hydroxyl group substituent than piceatannol resulting in a diminished antioxidant potency.
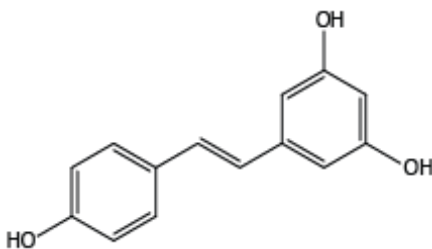
Figure 2.2: Structure of resveratrol.

Diethylstilbestrol was first synthesized to mimic estrogen and was prescribed to pregnant woman in the mid-1900's to aid in pregnancy complications.[7] In the early 1970's, diethylstilbestrol was found to be an endocrine disruptor, classified as a carcinogen, and ultimately prohibited.[7] Diethylstilbestrol, shown in Figure 2.3, has the least number of hydroxyl substituents of the three compounds with only two, one on each ring, further lessening its antioxidant potency.
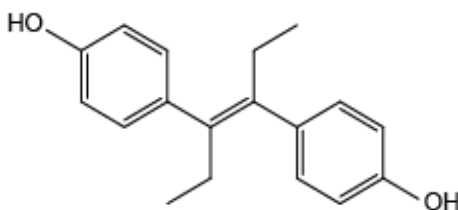
Figure 2.3: Structure of diethylstilbestrol.

The aim of this study was to investigate how the number of hydroxyl group substituents on stilbenoids affects the aggregation of Aβ.

2.3 Materials and Methods

2.3.1 Materials

Aβ(1-42) (>95% pure) was purchased from Atlantic Peptides (Scarborough, ME). Ethanol and sodium perchlorate were purchased from Sigma-Aldrich (St. Louis, MO) and used without further purification. Sodium phosphate monobasic, sodium phosphate dibasic, sodium chloride, and cyclohexane were purchased from Fisher Scientific (Pittsburgh, PA). Resveratrol, piceatannol, and diethylstilbestrol were purchased from Sigma-Aldrich (St. Louis, MO).

2.3.2 Amyloid- β (1-42) Protein Preparation

Aβ (1-42) (M.W. 4512.3 kDa) was dissolved in 10 mM sodium phosphate buffer, 20 mM NaCl, pH 7.4, sonicated for 10 min in an ice bath and centrifuged for 30 minutes at 14,000 rcf and 4°C (Centrifuge 5804 R, Eppendorf AG, Hamburg Germany). The concentration was estimated using the extinction coefficient of tyrosine, which is 1,280 $M^{-1}cm^{-1}$ at 280 nm using a Varian Cary Bio 50 UV-Vis spectrophotometer (Varian, Palo Alto, CA)[8]. Peptide concentrations ranged from 70-80 μM and were normalized in all the spectral processing. Aβ was prepared and incubated at 37°C over a 12-day time period. During this time, samples were analyzed every four days by CD and on Day 0 and Day 12 by dUVRR spectroscopy. Stock solutions of each polyphenolic compound were prepared in ethanol at a concentration of 5 mM. Polyphenolic compounds were then added to the protein solution for a final concentration of 25 μM. For dUVRR spectroscopy, sodium perchlorate was added to the sample as an internal intensity standard at a final concentration of 50 mM.

2.3.3 Circular Dichroism (CD)

A Jasco J-815 CD Spectropolarimeter (Jasco, Easton, MD) was used to collect CD spectra in the range of 190-250 nm. A scan speed of 50 nm/min with a response time of 4 sec was used. Five spectra were averaged for each sample. A 1 mm optical path length quartz cuvette (Hellman, Plainview, NY) was employed for all measurements.

2.3.4 Deep Ultraviolet Resonance Raman (dUVRR)

The dUVRR instrument has been described previously by *Wang et al.* [8] Briefly, UV light was generated using the fourth harmonic of a tunable 4 kHz frequency quadrupled Ti:Sapphire laser (Coherent Inc., Santa Clara, CA), which was pumped by a diode-pumped frequency doubled Nd:YLF laser (Coherent Inc., Santa Clara, CA). An excitation wavelength of 197 nm was employed for all measurements and the average power at the sample was attenuated to c.a. 500 µW to prevent sample degradation. The excitation light was directed towards the sample stream guided by two Nitinol wires. The sample was kept under N_2 gas to eliminated ambient oxygen, as O_2 has a feature at 1550 cm^{-1}. Spectra were calibrated using a cyclohexane spectrum and 50 mM sodium perchlorate was used as an internal intensity standard.

2.3.5 Data Analysis

Data analysis was carried out in the MATLAB R2016b (MathWorks, Natick, MA) environment. For all dUVRR spectra, the background buffer spectrum was subtracted and cosmic spikes were removed using an in-house cosmic ray removal algorithm. A nonlinear least-squares (NLLS) algorithm was used to fit each spectrum with a series of

Gaussian/Lorentzian bands, which approximate the Voigt line shape, as described previously.[9] All dUVRR spectra are the average of triplicate trials.

The amide I mode was deconvoluted into two peaks at 1657 and 1670 cm^{-1}. The amide II mode was centered at 1559 cm^{-1}, and the amide S mode was centered 1400 cm^{-1}. The amide III mode was deconvoluted into three bands at 1244, 1275, and 1311 cm^{-1}. Aβ has one tyrosine and three phenylalanines. It is likely that the tyrosine mode at 1263 cm^{-1} also contributes to the intensity of the amide III bands. Other tyrosine modes that show up in the dUVRR spectrum of Aβ include the fermi doublet (Y1) fitted at 820 and 858 cm^{-1}. The band at 820 cm^{-1} is about 10 cm^{-1} lower than expected, which is likely due to the high noise level at this region. The fitted peak at 1191 cm^{-1} is an overlapping phenylalanine and tyrosine mode (F/Y9a) that arises from C-H bending. The ring stretching modes of phenylalanine and tyrosine are also overlapped with combined bonds at 1213 and 1608 cm^{-1}. The feature at 936 cm^{-1} is from perchlorate, which was added as an internal intensity standard. A sharp feature at 1441 cm^{-1} is present in some spectra because TFA was added as a counter ion during the purification of early batches of the synthetic Aβ. The counter ion was later replaced by hydrochloride to remove this peak from the spectra. Difference spectra were created by subtraction of dUVRR spectra of Aβ from spectra of samples treated with polyphenols at each time point (Days 0 and 12). The difference spectra were multiplied by ten to better visualize the differences. Further difference spectra were created by subtraction of Day 0 dUVRR spectra from Day 12 dUVRR spectra to visualize the structural impact of the polyphenols made on the protein over time in the aromatic regions.

All CD spectra were averaged and the background buffer spectrum was subtracted from the raw data. The mean residue ellipticity (θ_{MRE}) was calculated using Equation 1 with ϑ being the raw ellipticity from the measurement (degrees), *MW* being the molecular weight of the protein (g/mol), *n* being the number of protein residues, *d* being the path length of the cell (cm), and *C* being the concentration of the sample (M).[8-10] All spectra are averaged spectra of triplicate trials.

Equation 1:
$$[\theta_{MRE}] = \frac{\theta \cdot MW}{10 \cdot n \cdot d \cdot C}$$

2.4 Results

2.4.1 Aβ Untreated

Figure 2.4 shows the CD spectra of Aβ during the 12-day incubation period. Initially on Day 0, the protein is disordered in structure, as indicated by the minimum at 197 nm. Over time, this feature decreases in intensity and another minimum is formed at 217 nm, indicative of β-sheet formation.
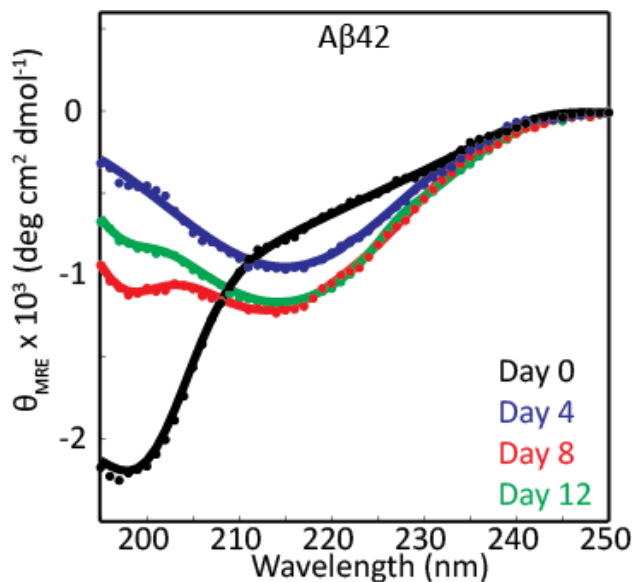
Figure 2.4: CD spectra of Aβ42 during a 12-day incubation period; Day 0 (black), Day 4 (blue), Day 8 (red), and Day 12 (green).

2.4.2 Piceatannol

Figure 2.5 shows the CD spectra of Aβ treated with piceatannol during the 12-day incubation period. Initially on Day 0, the protein is disordered in structure, as indicated by the minimum at 197 nm. There is a slight loss of intensity at 197 nm on Day 4 but over time, the protein remains in a disordered state with no additional changes in structure. Thus, the addition of piceatannol prevents the protein from forming β-sheet structure.

Figure 2.5: *CD spectra of Aβ42 treated with piceatannol during a 12-day incubation period; Day 0 (black), Day 4 (blue), Day 8 (red), and Day 12 (green).*

Figure 2.6 shows the dUVRR spectra of the Aβ protein treated with piceatannol on Day 0 when it was prepared and almost two weeks later on Day 12. The spectra were deconvoluted with each peak representing an amide or aromatic mode in the protein. Over time, there is no observable change in the spectra, however key differences are highlighted through difference spectra shown later.

Figure 2.6: Deconvoluted dUVRR spectra of Aβ42 treated with piceatannol on Days 0 and 12 (purple). Deconvolution of the individual amide and aromatic modes was performed and those peaks are shown under each spectrum.

Figure 2.7 shows the overlaid spectra of untreated Aβ and Aβ treated with piceatannol on Days 0 and 12. Differences are seen in amide III at 1244 cm^{-1}, amide S at 1400 cm^{-1}, and amide II at 1559 cm^{-1} which are stronger in the treated versus untreated spectrum on Day 12. Differences in the Y and F modes are seen predominantly in the Y modes at 820 and 858 cm^{-1}, and the Y/F modes at 1191, 1586, and 1608 cm^{-1}.
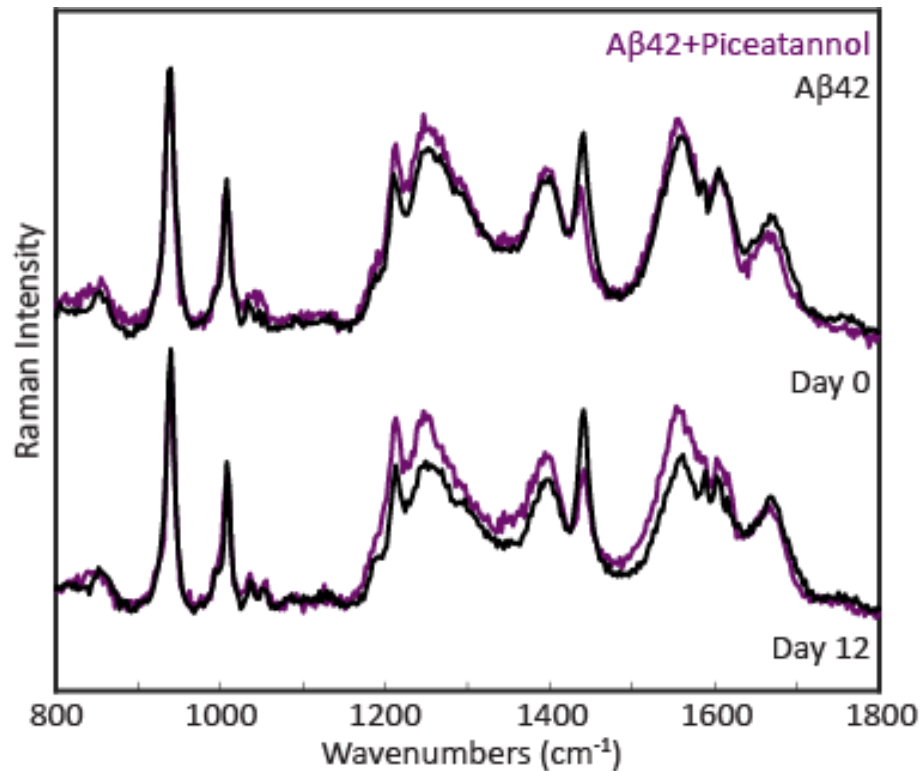
Figure 2.7: DUVRR spectra of Aβ42 (black) overlaid with Aβ42 treated with piceatannol (purple) on Days 0 and 12.

Figure 2.8 shows the difference between the untreated Aβ protein spectrum and the piceatannol-treated Aβ spectrum on Days 0 and 12. The difference spectra on Days 0 and 12 highlight that the amide modes are stronger in the dUVRR spectra of the treated samples. Modes associated with tyrosine at 858, 1191, 1213, and around 1608 cm^{-1} are increased in intensity in the dUVRR spectra of the treated samples. Interestingly, modes associated with phenylalanine at 1008, 1586, and 1608 cm^{-1} are decreased in intensity.
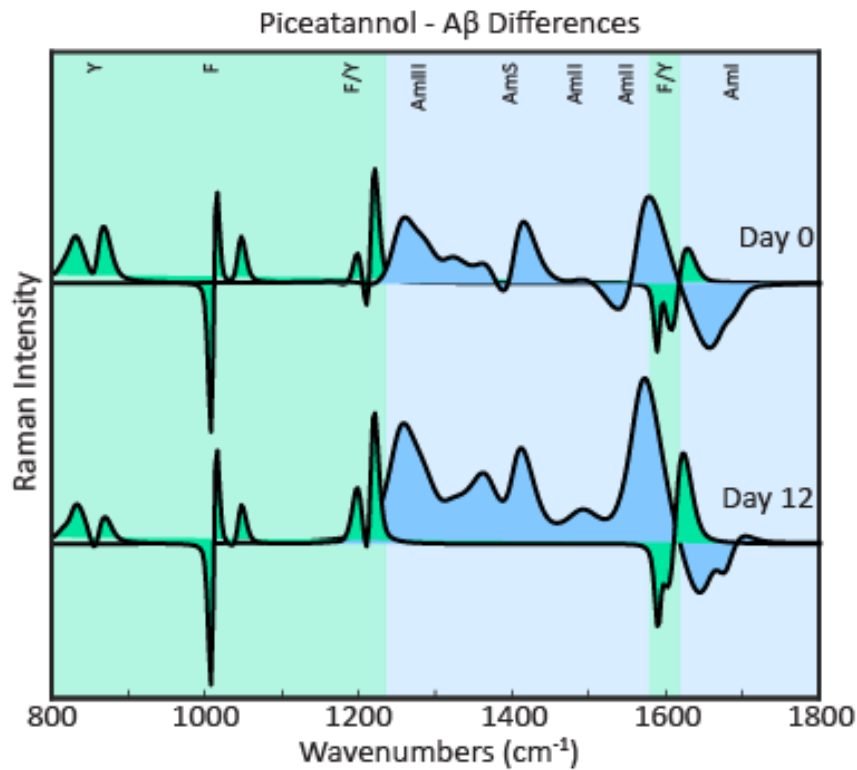
Figure 2.8: DUVRR difference spectra of the deconvoluted peaks of untreated Aβ42 and Aβ42 treated with piceatannol on Day 0 and Day 12. The amide modes are shown in blue and the aromatic modes are shown in green.

2.4.3 Resveratrol

Figure 2.9 shows the CD spectra of Aβ treated with resveratrol during the 12-day incubation period. Initially on Day 0, the CD spectrum indicates that the protein is disordered in structure as indicated by the strong minimum at 197 nm. The intensity of the minimum at 197 nm decreases with increasing incubation time, suggesting that the protein is changing structure. A small minimum begins to form at 217 nm by day 4, which is indicative of β-sheet structure. Addition of resveratrol does not prevent the Aβ from forming β-sheet structure during incubation. Resveratrol may slow the formation of β-sheet structure, but ultimately it does not prevent aggregation.
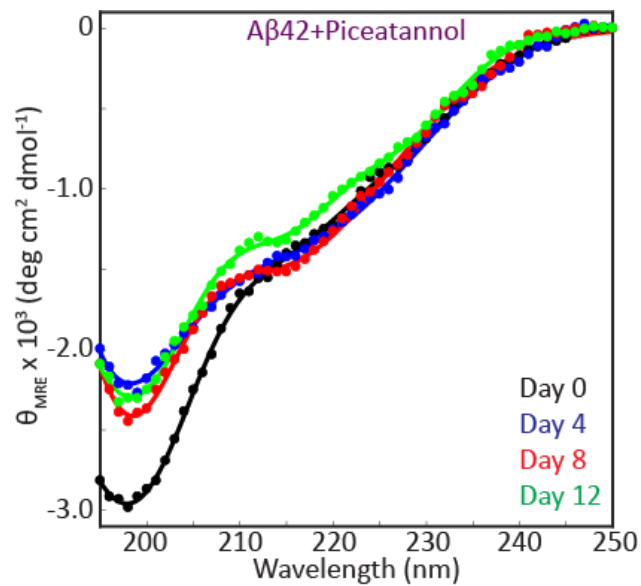

Figure 2.9: CD spectra of *Aβ42 treated with resveratrol during a 12-day incubation period; Day 0 (black), Day 4 (blue), Day 8 (red), and Day 12 (green).*

Figure 2.10 shows the dUVRR spectra of the Aβ protein treated with resveratrol on Days 0 and 12. The spectra were deconvoluted in to a series of peaks that represent the amide and aromatic modes of the protein. Over the 12-day incubation period, there is no pronounced change in the spectra, however key differences are highlighted in the difference spectra shown later.

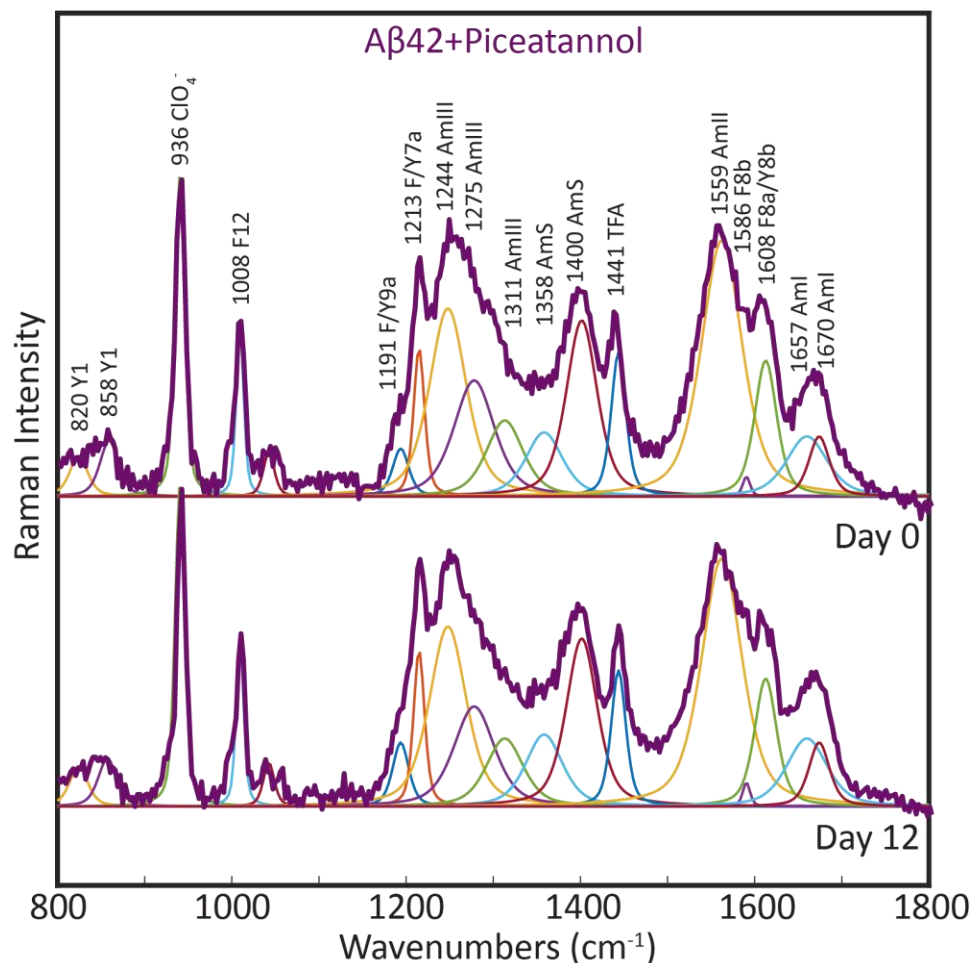*Figure 2.10: Deconvoluted dUVRR spectra of Aβ42 treated with resveratrol on Days 0 and 12 (pink). Deconvolution of the individual amide and aromatic modes was performed and those peaks are shown under each spectra.*

Figure 2.11 shows the overlaid dUVRR spectra of untreated Aβ and Aβ treated with resveratrol on Days 0 and 12. There are more differences between the Day 0 spectra than the Day 12 spectra. The CD spectra show that initially the protein is disordered, but it eventually forms β-sheet structure. The similarity of the Day 12 spectra suggest that any differences in structure initially between the two treatments are likely gone after 12 days of incubation.
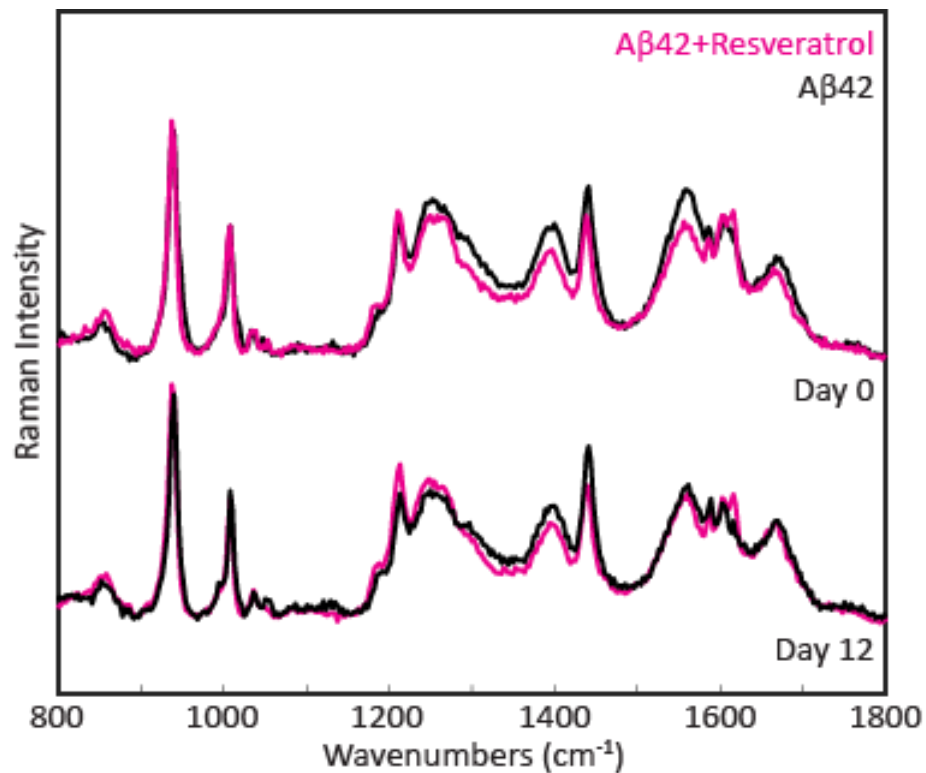
Figure 2.11: DUVRR spectra of Aβ42 (black) overlaid with Aβ42 treated with resveratrol (pink) on Days 0 and 12.

Figure 2.12 shows the difference spectra of the untreated Aβ protein and resveratrol-treated Aβ on Days 0 and 12. Initially there is a large difference in the intensity of the amide modes but this difference is reduced over time, likely due to the fact resveratrol does not prevent formation of β-sheet structure. The aromatic modes associated with tyrosine are stronger in the dUVRR spectra of Aβ treated with resveratrol but the phenylalanine modes at 1008 cm^{-1} is not.
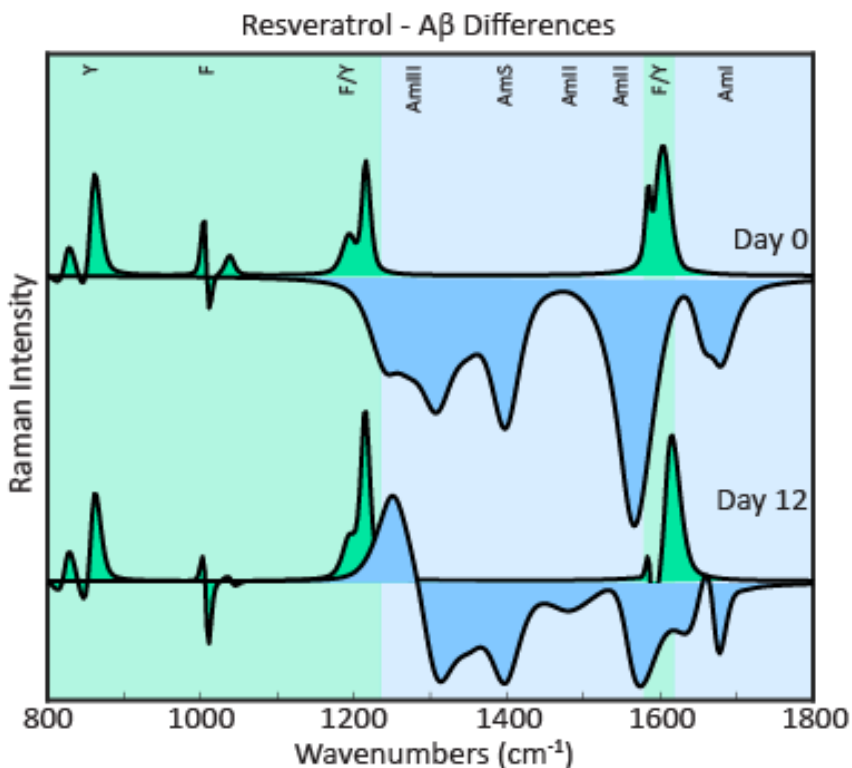
Figure 2.12: DUVRR difference spectra of the deconvoluted peaks of untreated Aβ42 and Aβ42 treated with resveratrol the untreated Aβ on Day 0 and Day 12. The amide modes are shown in blue and the aromatic modes are shown in green.

2.4.4 Diethylstilbestrol

Figure 2.13 shows the CD spectra of diethylstilbestrol-treated Aβ during the incubation period. Initially on Day 0, the CD spectrum indicates that the protein is largely disordered as indicated by the minimum at 197 nm. However, the CD spectrum quickly loses the negative feature at 197 nm and develops the characteristic β-sheet associated minimum at 217 nm. After Day 4, the CD spectrum remains stable indicating the structure of the protein remains unchanged for the rest of the incubation period.
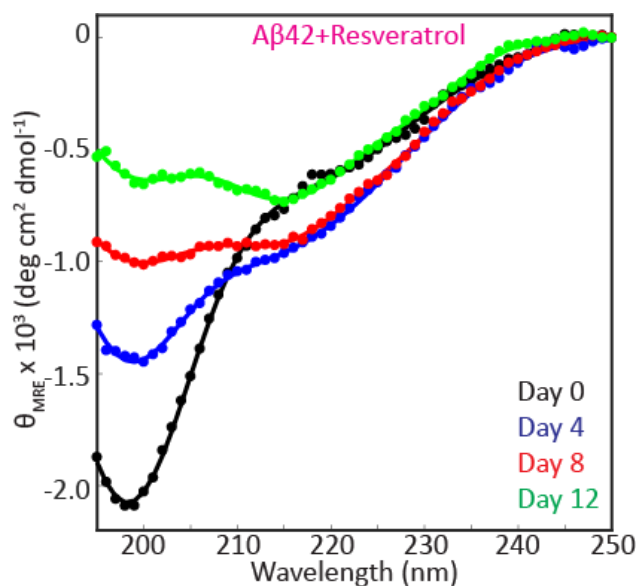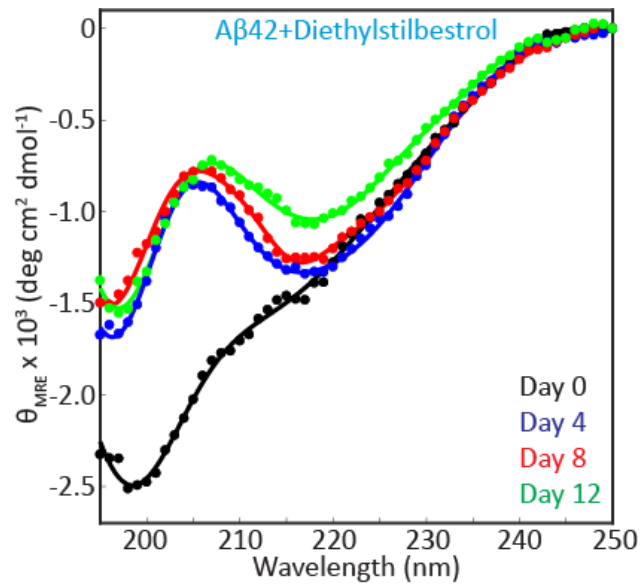

Figure 2.13: CD spectra of *Aβ42 treated with diethylstilbestrol during a 12-day incubation period; Day 0 (black), Day 4 (blue), Day 8 (red), and Day 12 (green).*

Figure 2.14 shows the dUVRR spectrum of the Aβ protein treated with diethylstilbestrol on Days 0 and 12.   With respect to the internal intensity standard perchlorate, the entire spectrum decreases in intensity. A decrease in overall intensity may be associated with formation of insoluble β-sheet oligomers.
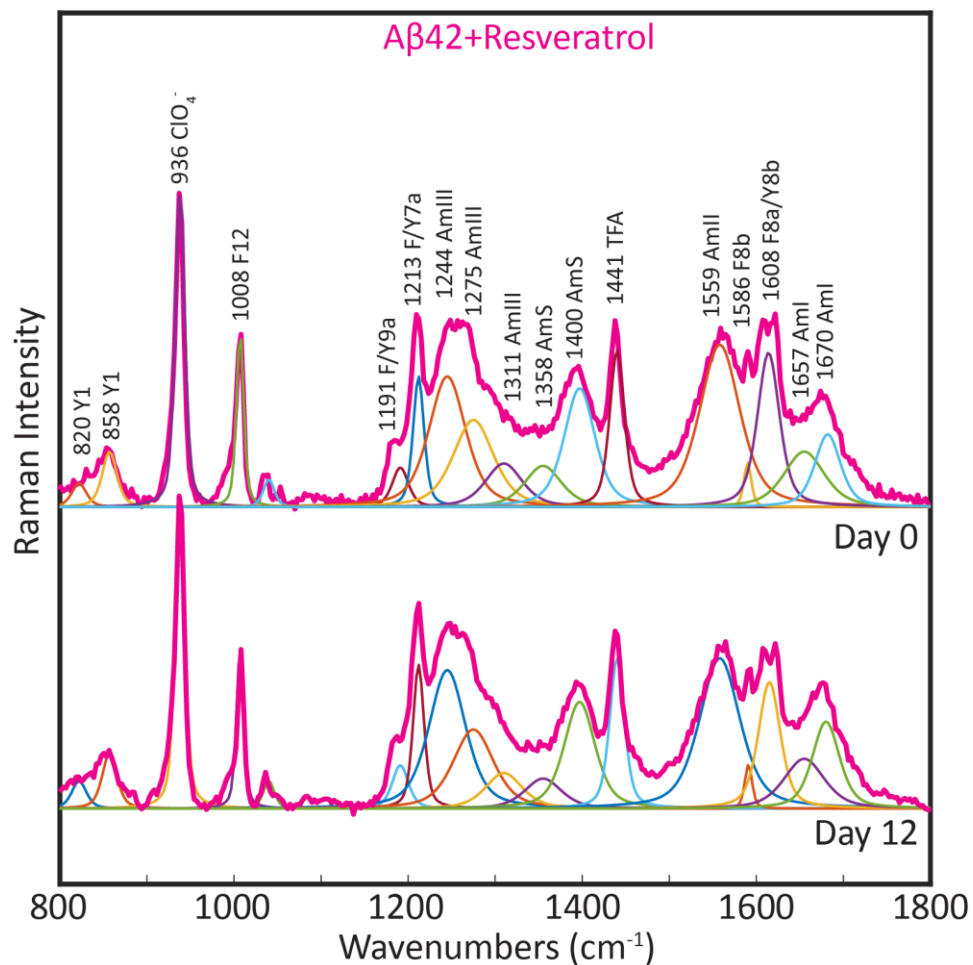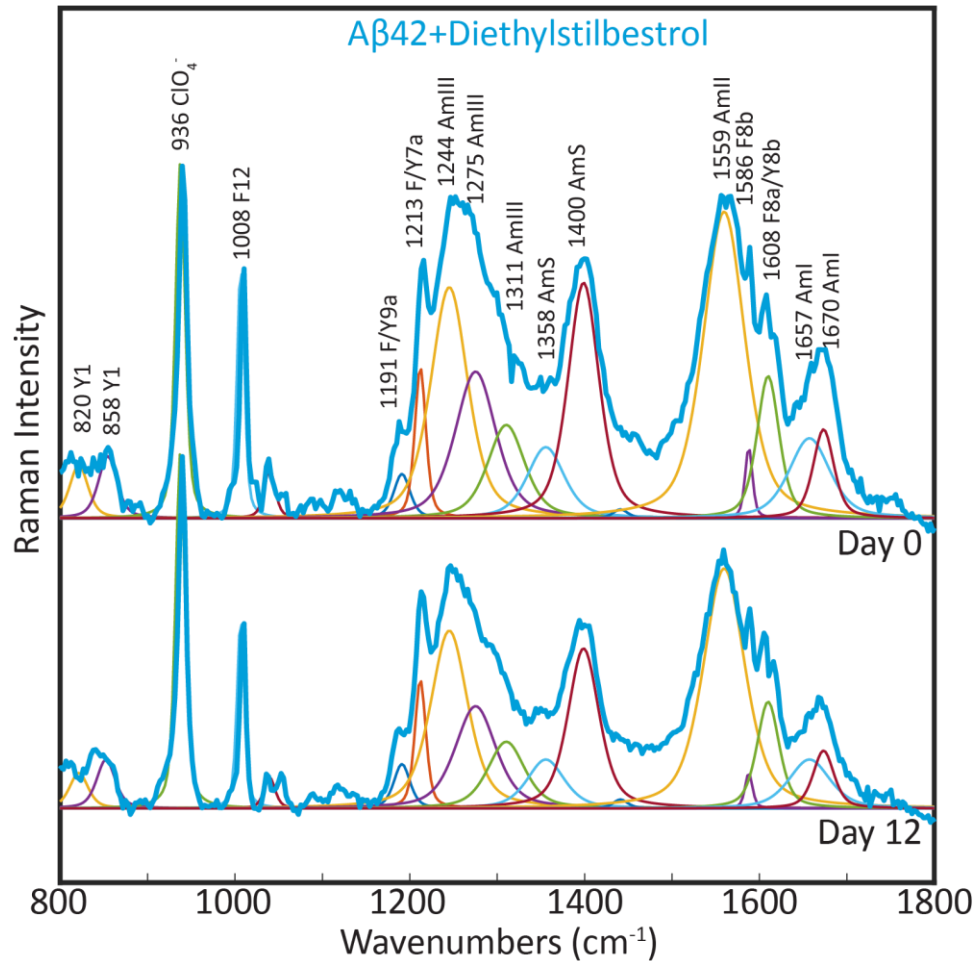

Figure 2.14: Deconvoluted dUVRR spectra of Aβ42 treated with diethylstilbestrol on Day 0 and Day 12 (blue). Deconvolution of the individual amide and aromatic modes was performed and those peaks are shown under each spectra.

Figure 2.15 shows the overlaid spectra of untreated Aβ42 and Aβ42 treated with diethylstilbestrol on Days 0 and 12. The most pronounced differences between the untreated and diethylstilbestrol-treated Aβ spectra are in the amide III and amide I regions. Differences in the aromatic modes of Y at 820 cm^{-1} and F at 1586 and 1608 cm^{-1} were also apparent. The spectrum of untreated Aβ also has a TFA peak that is not present in the diethylstilbestrol-treated sample spectrum, as the counter ion for the protein was changed to hydrochloride which does not have a feature in dUVRR spectra.
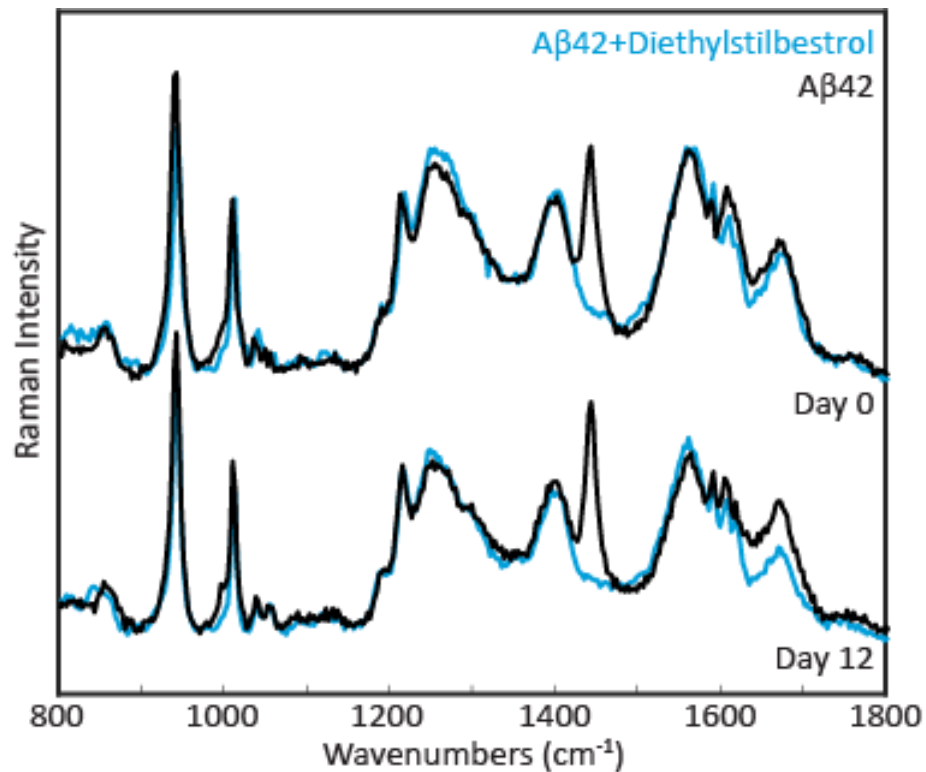
Figure 2.15: DUVRR spectra of Aβ42 (black) overlaid with Aβ42 treated with diethylstilbestrol (blue) on Days 0 and 12.

Figure 2.16 shows the difference spectra for the untreated Aβ protein and diethylstilbestrol-treated Aβ protein on Days 0 and 12. The amide II band at 1244 cm^{-1} is more intense suggesting the treated sample may have more β-sheet structure than the untreated sample initially. Interestingly, the amide I band is less intense. The aromatic bands are also decreased in intensity.
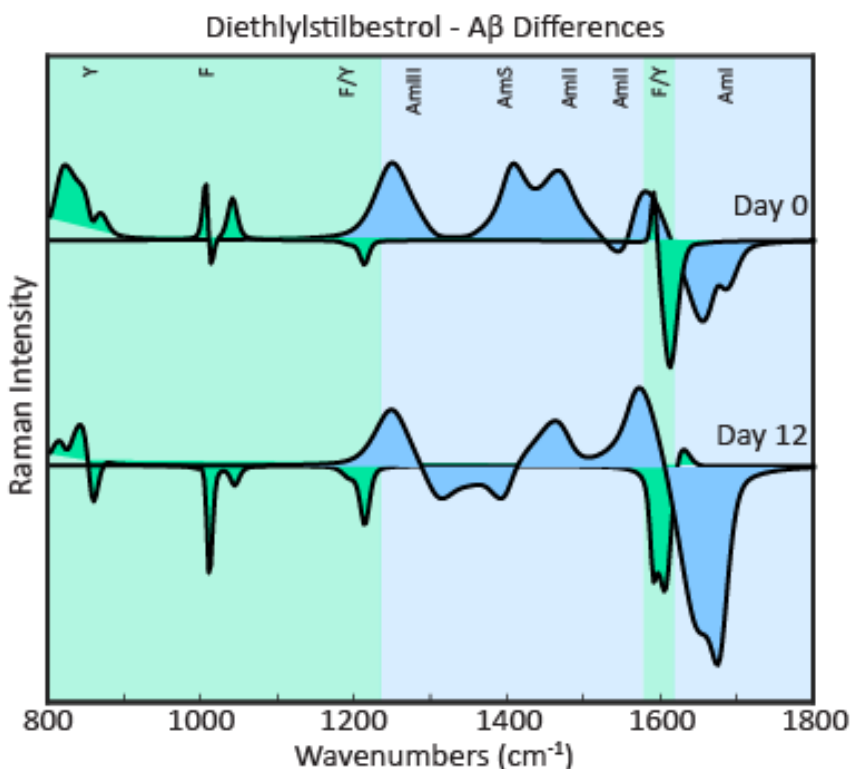
Figure 2.16: DUVRR difference spectra of the deconvoluted peaks of untreated Aβ42 and Aβ42 treated with diethylstilbestrol on Day 0 and Day 12. The amide modes are shown in blue and the aromatic modes are shown in green.

2.5 Discussion

The number of hydroxyl substituents on the rings of the stilbenoids used to treat Aβ samples appears to be positively correlated with the polyphenol's ability to prevent β-sheet formation. Specifically, more substituents on the rings of the stilbenoid traps the peptide in a disordered state as confirmed by CD. On Day 0, each of the polyphenol-

treated samples are disordered as evidenced by the strong negative feature at 197 nm in their CD spectra. By Day 4, the negative intensity at 197 nm is reduced in CD spectra of all samples, but to differing degrees. The piceatannol-treated sample remained largely disordered, while the sample treated with resveratrol has an observable amount of β-sheet structure. Samples treated with diethylstilbestrol lost their disordered structure completely by Day 4 and formed β-sheet structure.

As the number of hydroxyl substituents decrease, there is a trend in the effect on the aromatic modes as seen in Figure 2.17. The phenylalanine mode at 1008 cm^{-1} was most intense in the dUVRR spectrum of Aβ treated with piceatannol, which has the greatest number of hydroxyl substituents. As the number of hydroxyl substituents decreases, the intensity of the 1008 cm^{-1} band decreased. The overlapped ring stretching Y/F mode at 1213 cm^{-1} was increased in dUVRR spectra of samples treated with piceatannol or resveratrol but decreased in samples treated with diethylstilbestrol.

As the number of substituents on the rings of the stilbenoids decrease, aromatic modes mainly decrease in intensity. As the number of substituents increase, there appears to be less interaction between the stilbenoid and the aromatic residues of the protein. Decreasing the polarity of the chain linker may also yield a stronger interaction between the polyphenol and the aromatic residues of the protein. This is seen in Figure 2.17 where the aromatic modes are most perturbed in the dUVRR spectra of samples treated with diethylstilbestrol. Decreasing the number of substituents, reduces the polarity of the polyphenol. This may be allowing for more pi-stacking interactions with

the protein yielding greater changes in the aromatic bands than when more hydroxyl

groups are present on the ring.
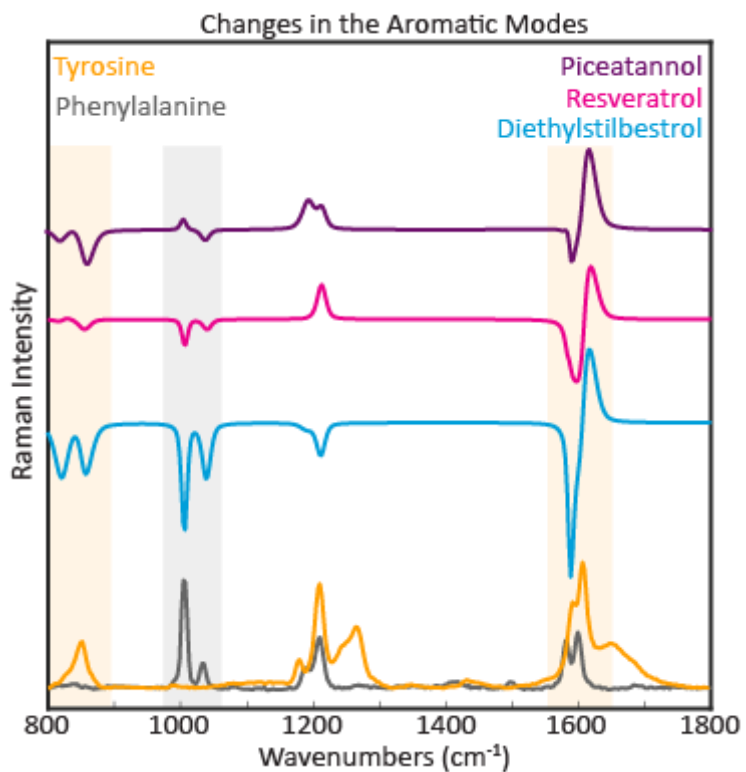
Figure 2.17: Changes over the 12-day incubation period in the individual aromatic modes of the dUVRR spectra. Diethylstilbestrol (blue), resveratrol (pink), and piceatannol (purple) are shown.

2.6 References

1. Lakey-Beitia, J.; Berrocal, R.; Rao, K. S.; Durant, A. A., Polyphenols as therapeutic molecules in Alzheimer's disease through modulating amyloid pathways. *Mol Neurobiol* **2015,** *51* (2), 466-479.

2. Porat, Y.; Abramowitz, A.; Gazit, E., Inhibition of amyloid fibril formation by polyphenols: structural similarity and aromatic interactions as a common inhibition mechanism. *Chem Biol Drug Des* **2006,** *67* (1), 27-37.

3. Gauci, A. J. C., M.; Giese, A.; Scerri, C.; Vassallo, V. , Identification of polyphenolic compounds and black tea extract as potent inhibitors of lipid membrane destabilization by A beta(42) aggregates - ResearchGate. *J of Alz Dis* **2011,** *24* (4), 767-779.

4. Ono, K.; Yoshiike, Y.; Takashima, A.; Hasegawa, K.; Naiki, H.; Yamada, M., Potent anti-amyloidogenic and fibril-destabilizing effects of polyphenols in vitro: implications for the prevention and therapeutics of Alzheimer's disease. *J Neurochem* **2003,** *87* (1), 172-181.

5. Lai, N. H.; Herent, M. F.; Leclercq, J. Q.; Nguyen, B. T.; Rogez, H.; Larondelle, Y.; Andre, C. Piceatannol, a potent bioactive stilbene, as major phenolic component in *Rhodomyrtus tomentosa*. *Food Chem* **2013,** *138 (2-3),* 1421-1430.

6. Burns, J.; Yokota, T. ; Ashihara, H.; Lean M. E.; Crozier, A. Plant foods and herbal sources of resveratrol. *J Agric Food Chem* **2002,** *50 (11),* 3337-3340.

7. Adam, E.; Decker, D. G.; Herbst, A. L.; Noller, K. L.; Tilley, B. C.; Townsend, D. E. Exposure in utero to diethylstilbestrol and related synthetic hormones: Association with vaginal and cervical cancers and other abnormalities. *JAMA* **1976,** *236 (10),* 1107-1109.

8. Wang, M.; JiJi, R.D. Spectroscopic detection of β-sheet structure in nascent Aβ oligomers. *J Biophotonics* **2011**, *4*, 637-644.

9. Simpson, J. V.; Balakrishnan, G.; JiJi, R. D. MCR-ALS analysis of two-way UV resonance Raman spectra to resolve discrete protein secondary structural motifs. *Analyst* **2009,** *134,* 138-147.

10. Wang, M.; JiJi, R. D. Resolution of localized small molecule-Aβ interactions by deep-ultraviolet resonance Raman spectroscopy. *Biophys Chem* **2011,** *158,* 96-103.

Chapter III: Increasing Chain Linker Polarity Increases β-sheet Formation

3.1 Abstract

Diaryl polyphenolic compounds have common structural components consisting of two phenolic rings with hydroxyl group substituents and a chain linker between the rings. The chain between the two phenol rings can vary significantly both in length and atom makeup, affecting the potency of the polyphenol. Flavonoid compounds do not contain a chain linker and understanding how the chain linker can affect the activity of non-flavonoid compounds is imperative. The aromatic rings of polyphenols are important for their binding to proteins and effects on protein aggregation. The type of linker between the aromatic rings of diaryl polyphenols is also important because it could affect Aβ binding and aggregation. The diaryl polyphenols nordihydroguaiaretic acid, curcumin, and rosmarinic acid have increasing polarity, respectively, in the chain linker between the phenolic rings. Each of these polyphenols has four ring substituents and 4 - 6 atoms in their chain linker. It this study, it was found that with increasing polarity of the linker, the polyphenol-treated Aβ sample had a greater tendency to form a β-structure. Thus, in order to maintain Aβ in a disordered structure (non-fibrillar), the linker between the phenol rings should be of low polarity. A polar linker leads to a reduction in disordered content and an increase in β-sheet structure in the protein.

3.2 Introduction

The chain linker between the two phenol rings can vary significantly both in length and atom makeup, and has an important impact on how the polyphenols will metabolize and behave.[1-2] It is suggested that the optimum chain length for inhibiting amyloid formation between the rings should be 2-6 atoms long.[3] Studies have shown that diaryl polyphenols such as curcumin, are better than flavonoids at inhibiting Aβ's amyloidogenic activity, possibly due to the type of chain linker between the aromatic rings.[1-2]

The aromatic rings are important for polyphenol binding to proteins and for inhibiting protein aggregation. The aromatic rings of polyphenols participate in hydrophobic interactions with proteins that can interrupt endogenous hydrophobic interactions within the protein. The endogenous interactions promote aggregation of Aβ by maintaining its stability and orienting the protein for self-assembly of organized structures.[3, 4-9] The rings of polyphenols have the necessary planarity to bind to the protein in the hydrophobic groove, interrupt the π stacking, and preventing aggregation by intercalating within the β-sheets.[1, 4, 10-11] The chain linker polarity will affect the polyphenol's overall polarity and its ability to disrupt hydrophobic interactions necessary for protein aggregation.

The polyphenols nordihydroguaiaretic acid, curcumin, and rosmarinic acid have increasing polarity, respectively, within the chain linker region between their phenolic rings. Each of these polyphenols have four ring substituents and 4 - 6 atoms in their chain linker.

Nordihydroguaiaretic acid is a plant based polyphenol found in the leaves of a desert shrub, the creosote bush and is valued for its anti-inflammatory effects.[12] Nordihydroguaiaretic acid, shown in Figure 3.1, is the least polar of the polyphenols evaluated in this study. It has four atoms in the chain linker between the rings with two methyl substituents off the second and third carbons. It has a total of four hydroxyl groups on the rings as well.
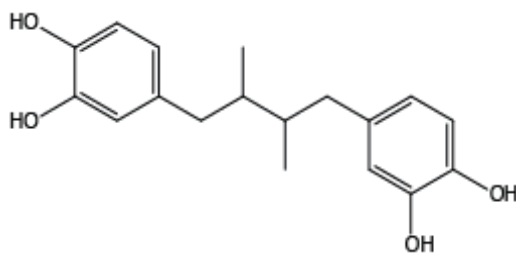
Figure 3.1: Structure of nordihydroguaiaretic acid.

Curcumin is the principal curcuminoid found in turmeric and has not only been used as a spice, but for its anticancer and anti-inflammatory effects as well.[13] Curcumin, shown in Figure 3.2, is more polar than nordihydroguaiaretic acid, but less polar than rosmarinic acid. It has five atoms in the chain linker between the rings with one hydroxyl substituent off the second carbon and a ketone off the fourth carbon. It has a total of two hydroxyl groups on the rings as well as two ether groups.
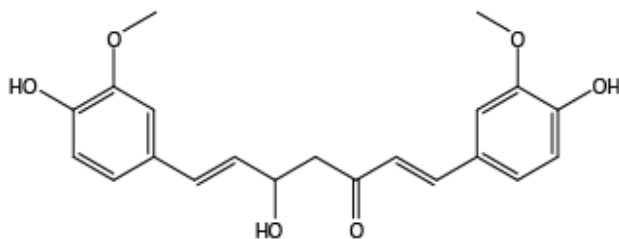
Figure 3.2: Structure of curcumin.

Rosmarinic acid is commonly found in many spices such as sage, mint, thyme, basil, and rosemary where it developed its name.[14] Rosmarinic acid, shown in Figure

3.3, is the most polar of the three polyphenols evaluated. It has six atoms in the chain

linker between the rings with an ester and carboxylic acid on the third and fourth

carbons, respectively.
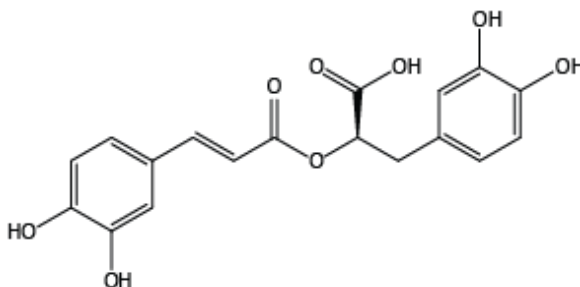
Figure 3.3: Structure of rosmarinic acid.

This study aims to discover how the polarity of the chain linker of polyphenols

can affect Aβ aggregation and β-sheet formation over time.

3.3 Materials and Methods

3.3.1 Materials

Aβ (1-42) (>95% pure) was purchased from Atlantic Peptides (Scarborough, ME).

Ethanol and sodium perchlorate were purchased from Sigma-Aldrich (St. Louis, MO) and

used without further purification. Sodium phosphate monobasic, sodium phosphate

dibasic, sodium chloride, and cyclohexane were purchased from Fisher Scientific

(Pittsburgh, PA). Rosmarinic acid and nordihydroguaiaretic acid were purchased from

Sigma-Aldrich (St. Louis, MO) and curcumin was purchased from Acros Organics

(Pittsburgh, PA).

3.3.2 Spectroscopic Measurements and Data Analysis

The amyloid-β (1-42) protein was prepared and characterized as described in

Chapter 2, section 2.3.2. Circular dichroism (CD) and deep-ultraviolet resonance Raman

(dUVRR) were collected, processed, and analyzed as described in Chapter 2, sections 2.3.3-2.3.5.

3.4 Results

3.4.1 Aβ Untreated

Figure 3.4 shows the CD spectra of Aβ during the 12-day incubation period. Initially on Day 0, the protein is a disordered in structure, as indicated by the minimum at 197 nm. Over time, this feature decreases in intensity and another minimum forms at 217 nm indicative of β-sheet formation.
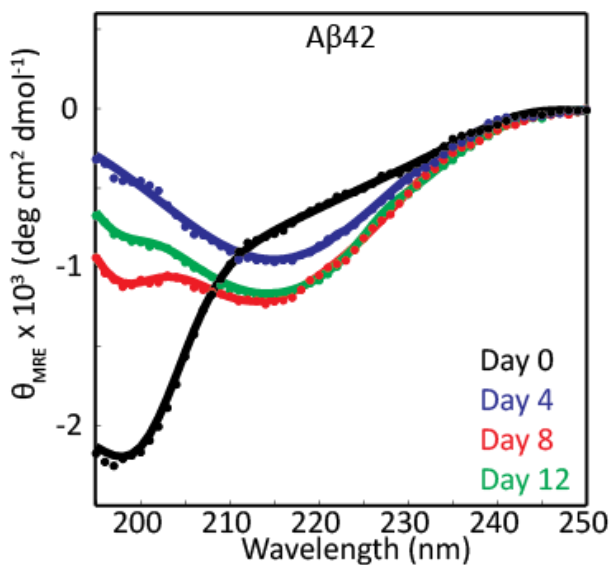
Figure 3.4: CD spectra of Aβ42 during a 12-day incubation period; Day 0 (black), Day 4 (blue), Day 8 (red), and Day 12 (green).

3.4.2 Nordihydroguaiaretic Acid

Figure 3.5 shows the CD spectra of nordihydroguaiaretic acid-treated Aβ during the incubation period. Similar to the untreated Aβ sample, on Day 0, the treated protein is a disordered in structure, as indicated by the minimum at 197 nm. There is a slight loss of intensity at 197 nm on Day 4 but over time, the structure of the treated protein remains stable and disordered.
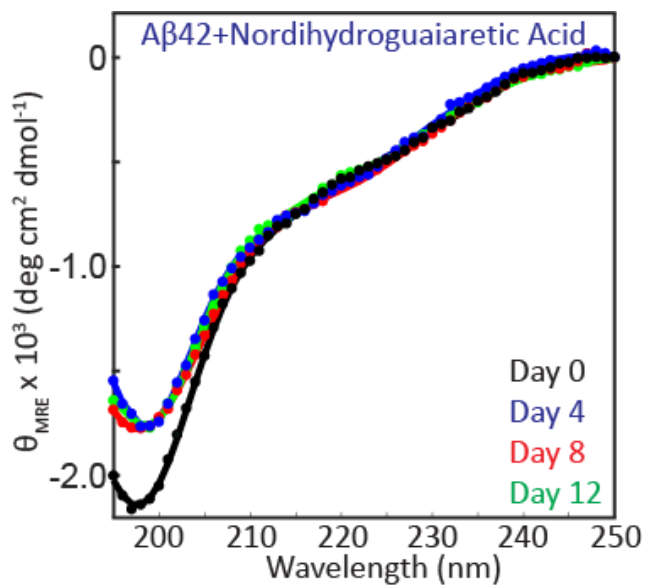
Figure 3.5: *CD spectra of Aβ42 treated with* nordihydroguaiaretic acid *during a 12-day incubation period; Day 0 (black), Day 4 (blue), Day 8 (red), and Day 12 (green).*

Figure 3.6 shows the Aβ protein treated with nordihydroguaiaretic acid on Days

0 and 12. The most noteworthy difference is the peak at 1295 cm^{-1}. This extra peak is

attributed to the stretching of the hydroxyl groups on the rings of the polyphenol itself.

Over time, there is no visible change between the Day 0 and Day 4 dUVRR spectra other

than this peak from nordihydroguaiaretic acid. After 12 days, this peak disappears due

to the oxidation of the polyphenol. The hydroxyl groups donate a hydrogen to the

protein which could be crucial in preventing protein aggregation. Observing this peak

on Day 0 and not on Day 12 confirms that the polyphenol is undergoing oxidation.
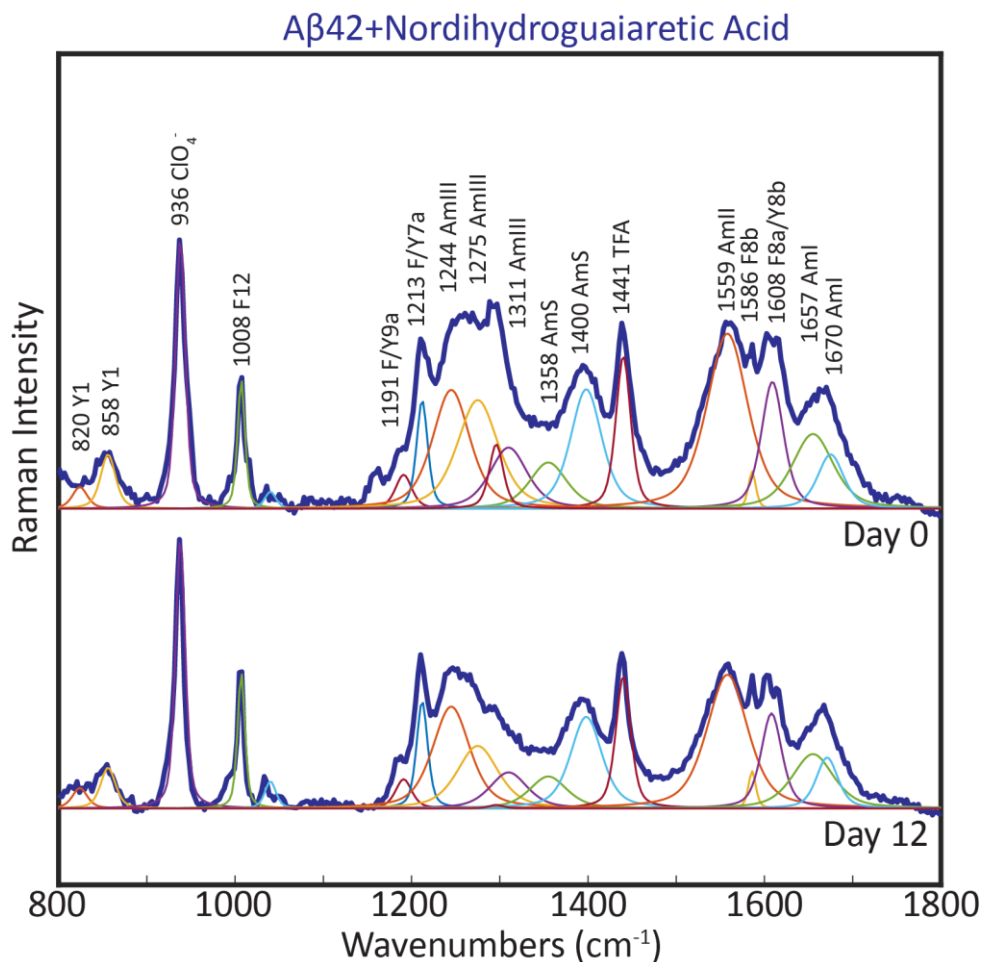
Figure 3.6: Deconvoluted dUVRR spectra of Aβ42 treated with nordihydroguaiaretic acid on Days 0 and 12 (blue). Deconvolution of the individual amide and aromatic modes was performed and those peaks are shown under each spectra.

Figure 3.7 shows the overlaid spectra of untreated Aβ and Aβ treated with nordihydroguaiaretic acid on Days 0 and 12. The most pronounced difference between the untreated and treated Aβ dUVRR spectra is the peak at 1295 cm^{-1} from the polyphenol. Other differences include a slight increase in the intensity of the F/Y modes at 1586 and 1608 cm^{-1} as well as the Y mode at 858 cm^{-1} for the treated sample.
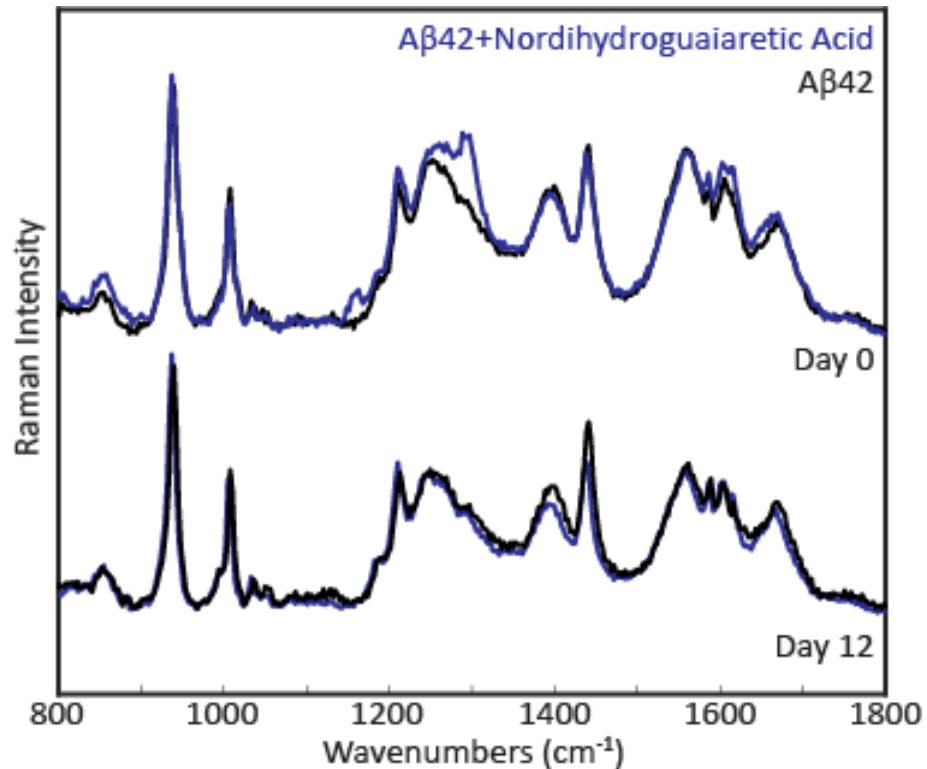
Figure 3.7: DUVRR spectra of Aβ42 (black) overlaid with Aβ42 treated with nordihydroguaiaretic acid (blue) on days 0 and 12.

Figure 3.8 shows the differences between the untreated Aβ protein and the nordihydroguaiaretic acid-treated Aβ dUVRR spectra on Days 0 and 12. The largest difference between the Day 0 spectra is in the amide III region, which is primarily due to the loss of the 1295 cm^{-1} peak from the polyphenol. On Day 0, tyrosine associated modes appear to be stronger in the spectrum of the treated Aβ sample, but the phenylalanine mode at 1008 cm^{-1} appears to have lower intensity. By Day 12, the differences in the aromatic modes have diminished.
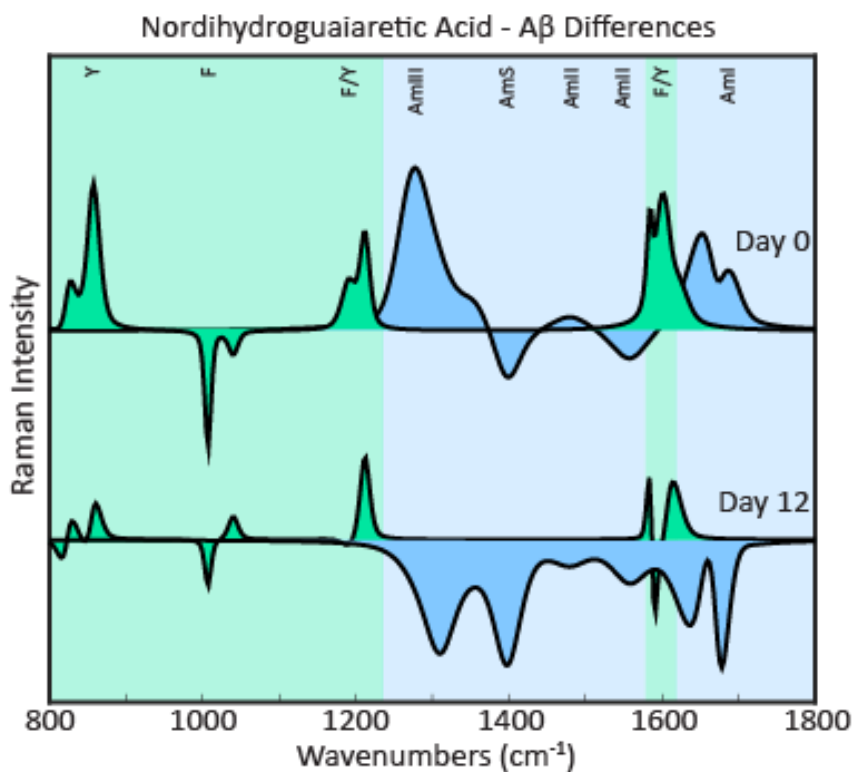
Figure 3.8: DUVRR difference spectra of the deconvoluted peaks of Aβ42 treated with nordihydroguaiaretic acid and the untreated Aβ42 on Day 0 and Day 12. The amide modes are shown in blue and the aromatic modes are shown in green.

3.4.3 Curcumin

Figure 3.9 shows the CD spectra of curcumin-treated Aβ during the incubation period. Initially on Day 0, the curcumin-treated protein is disordered in structure, as indicated by the minimum at 197 nm. Although there is a slight loss of intensity at 197 nm after each time point, the treated protein remains in disordered state.

Figure 3.9: CD spectra of *Aβ42 treated with* curcumin *during a 12-day incubation period; Day 0 (black), Day 4 (blue), Day 8 (red), and Day 12 (green).*

Figure 3.10 shows the dUVRR spectra of the Aβ protein treated with curcumin on Days 0 and 12. Difference spectra are needed to observe any changes that are occurring. The F/Y modes at 1589 and 1611 cm^{-1} are visibly different between Days 0 and 12.

Figure 3.10: Deconvoluted dUVRR spectra of Aβ42 treated with curcumin on Days 0 and 12 (green). Deconvolution of the individual amide and aromatic modes was performed and those peaks are shown under each spectra.

Figure 3.11 shows the overlaid spectra of curcumin treated and untreated Aβ samples on Days 0 and 12. The differences between the dUVRR spectra of the untreated and treated Aβ samples on Day 0 are predominately limited to the aromatic ring modes at 1213, 1589, and 1611 cm^{-1}. On Day 12, the Aβ sample differs from the curcumin-treated sample spectrum in the amide I, II, and III modes. Overall, the amide I, II, and III modes are less intense.
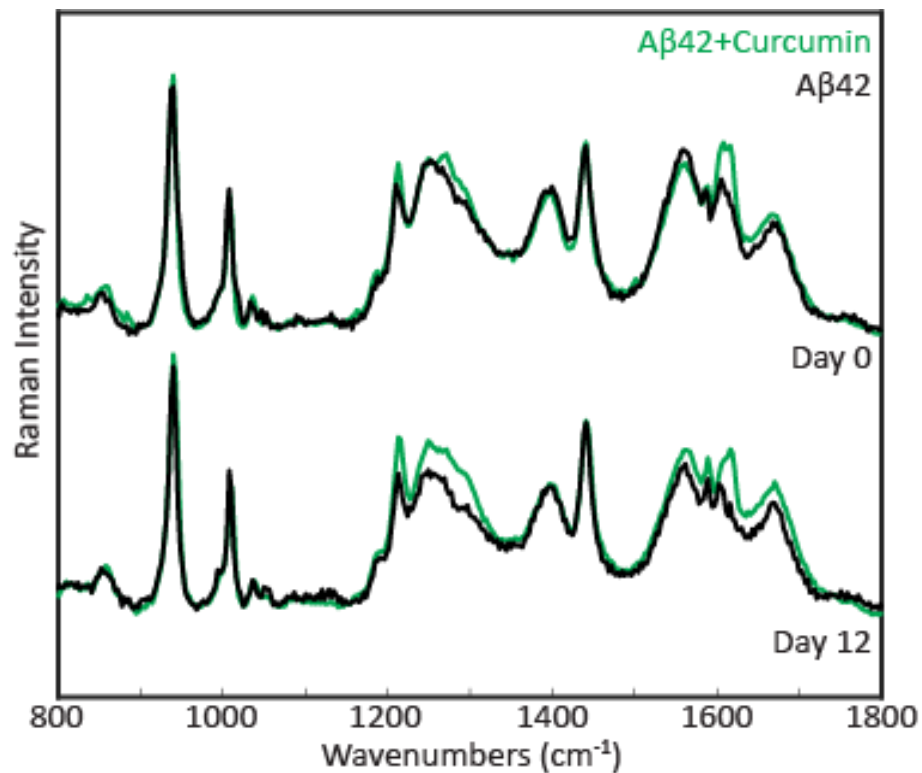
Figure 3.11: DUVRR spectra of Aβ42 (black) overlaid with Aβ42 treated with curcumin (green) on Days 0 and 12.

Figure 3.12 shows the difference between the untreated Aβ protein and the curcumin treated Aβ dUVRR spectra on Days 0 and 12. Initially on Day 0, the fitted aromatic modes are more intense in the spectrum of the treated sample. By Day 12, differences in the amide regions are observed due to differences in the structure of the protein between the untreated and curcumin-treated samples.

Figure 3.12: DUVRR difference spectra of the deconvoluted peaks of Aβ42 treated with curcumin and the untreated Aβ42 on Day 0 and Day 12. The amide modes are shown in blue and the aromatic modes are shown in green.

3.4.4 Rosmarinic Acid

Figure 3.13 shows the CD spectra of rosmarinic acid-treated Aβ during the 12-day incubation period. On Day 0, the protein is disordered in structure, as indicated by the minimum at 197 nm. Although the protein remains disordered in structure over time, there is a loss of intensity at 197 nm, and a minimum at 217 nm begins to develop.
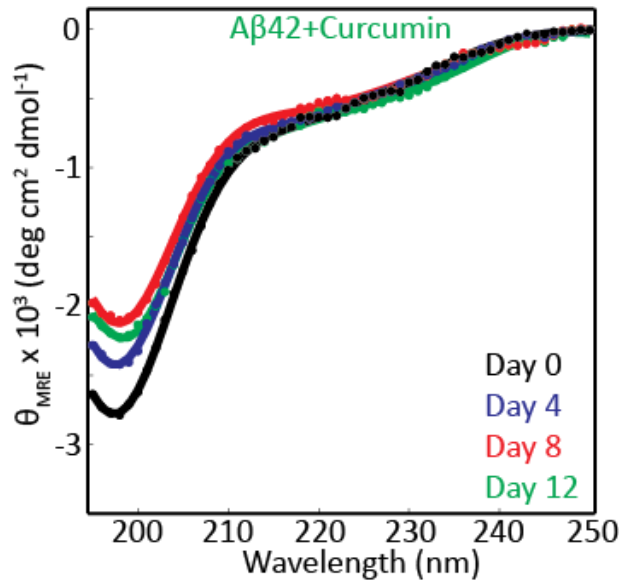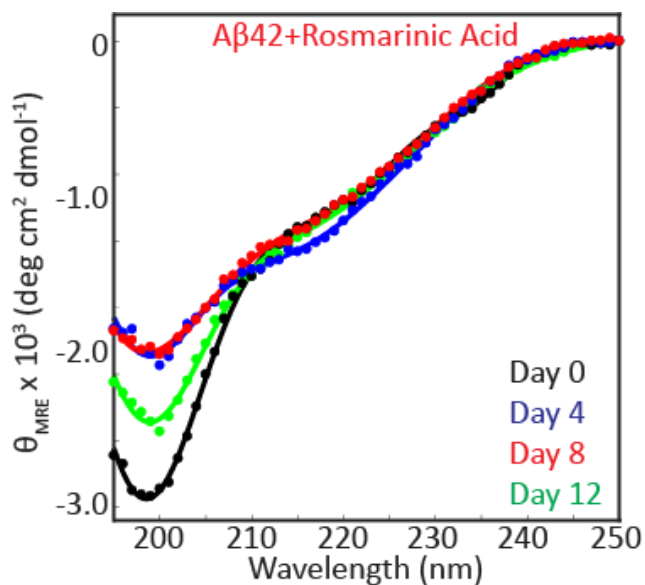

Figure 3.13: CD spectra of *Aβ42 treated with* rosmarinic acid *during a 12-day incubation period; Day 0 (black), Day 4 (blue), Day 8 (red), and Day 12 (green).*

Figure 3.14 shows the dUVRR spectra of the Aβ protein treated with rosmarinic acid on Days 0 and 12. There is a visible loss of intensity in the amide III mode at 1275 cm^{-1} and the amide I mode at 1654 and 1678 cm^{-1}. There are also changes in the aromatic modes at 1586 and 1608 cm^{-1}.
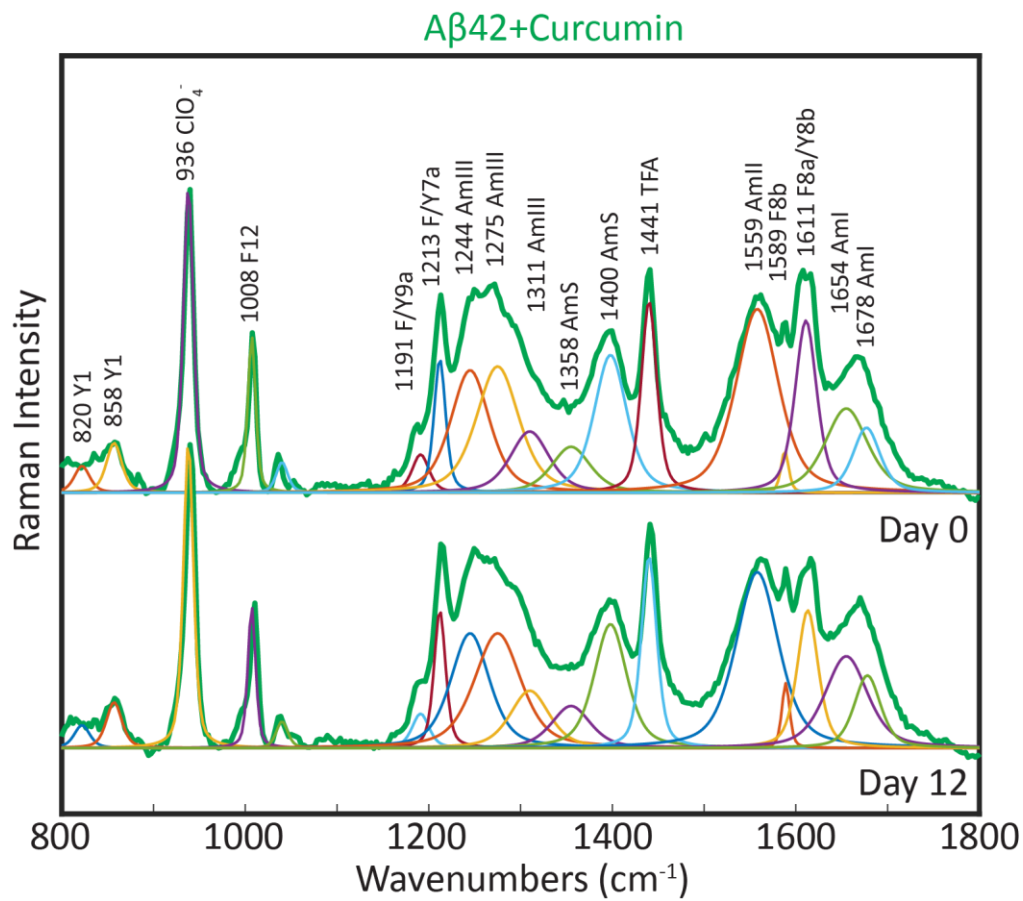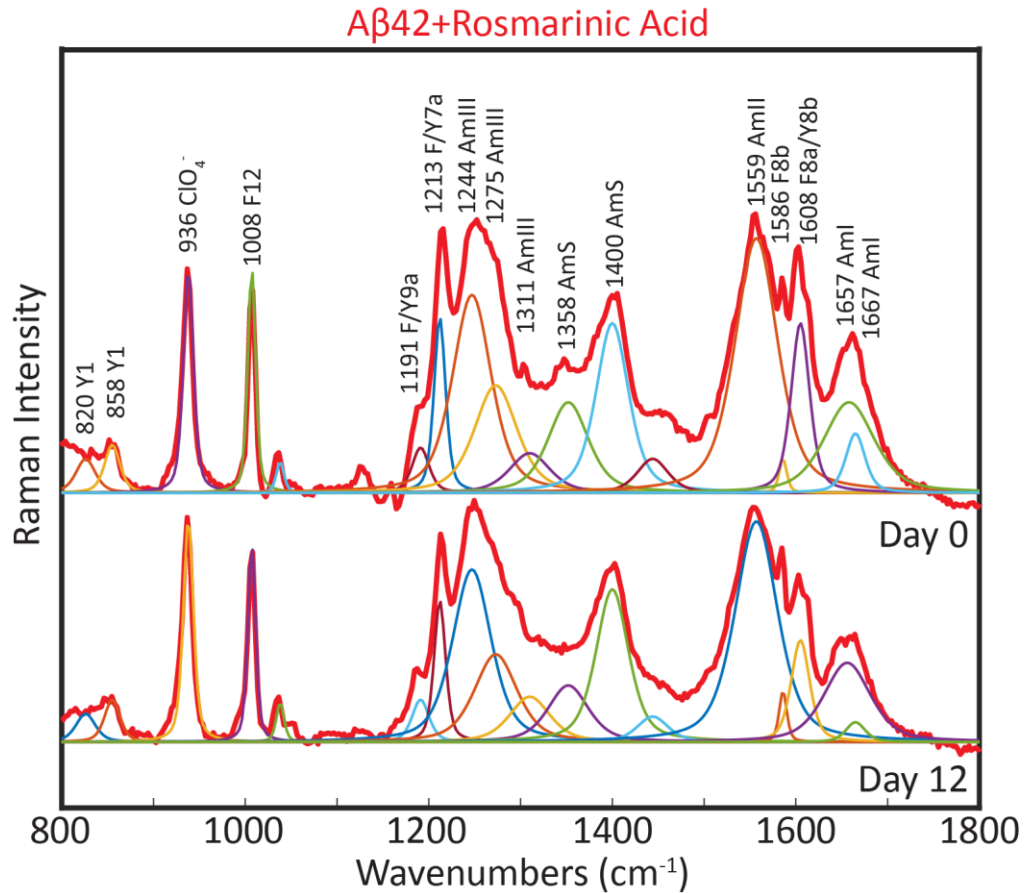

Figure 3.14: Deconvoluted dUVRR spectra of Aβ42 treated with rosmarinic acid on Days 0 and 12 (red). Deconvolution of the individual amide and aromatic modes was performed and those peaks are shown under each spectra.

Figure 3.15 shows the overlaid spectra of Aβ treated with rosmarinic acid protein and the untreated protein sample on Days 0 and 12. The most pronounced difference between the untreated and treated Aβ spectra is the peak in the amide III region around 1295 cm^{-1}. Loss of intensity in this region without a concurrent decrease in the amide III intensity at 1244 cm^{-1}, may suggest a greater proportion of β-structure in the samples treated with rosmarinic acid. The strong feature at 1441 cm^{-1} arises from TFA, as mentioned earlier. Addition of rosmarinic acid also results in a decrease in the amide I mode at 1657 and 1667 cm^{-1} and the F/Y modes at 1586 and 1608 cm^{-1}.
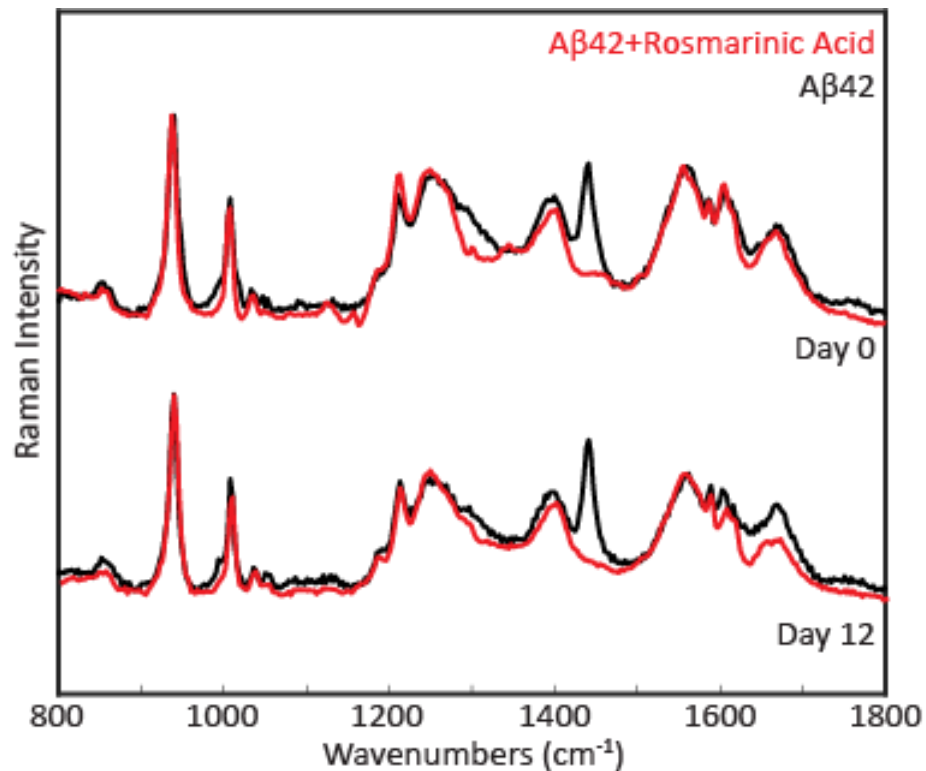
Figure 3.15: DUVRR spectra of Aβ42 (black) overlaid with Aβ42 treated with rosmarinic acid (red) on Days 0 and 12.

Figure 3.16 shows the differences between the dUVRR spectra of the untreated

Aβ protein and rosmarinic acid-treated Aβ on Days 0 and 12. Initially, the differences are

predominantly located in the amide regions. Specifically, the amide III band at 1295 cm^{-1}

appear lower in intensity suggesting a structural difference. By Day 12, the amide III and

II modes are stronger in the dUVRR spectrum of the treated sample. Small differences in

the F/Y modes at 1586 and 1608 cm^{-1} and the F mode at 1008 cm^{-1} are also observed
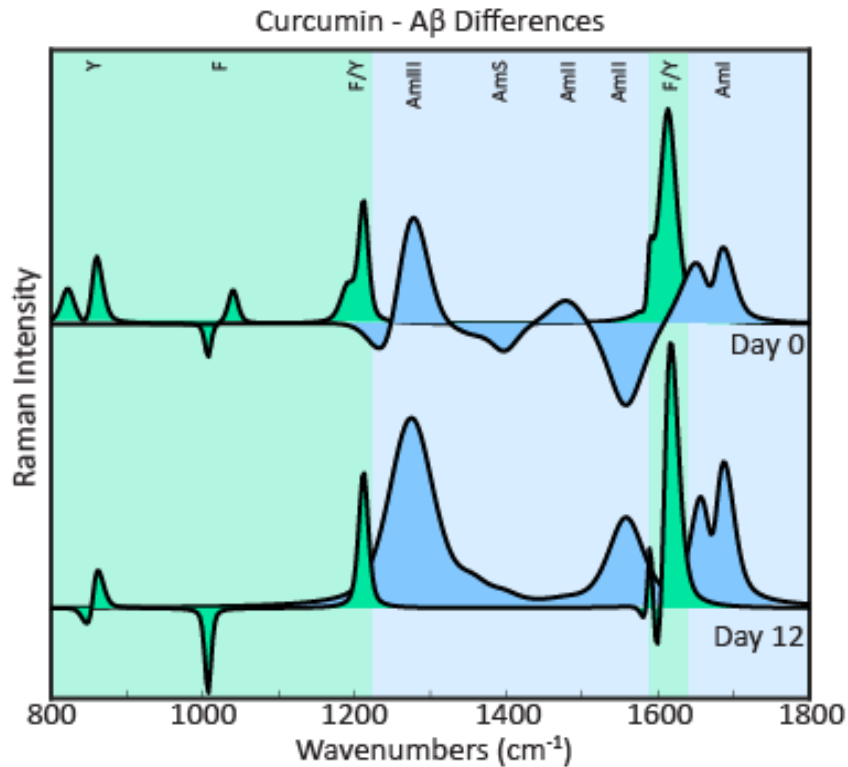
upon rosmarinic acid treatment of Aβ.
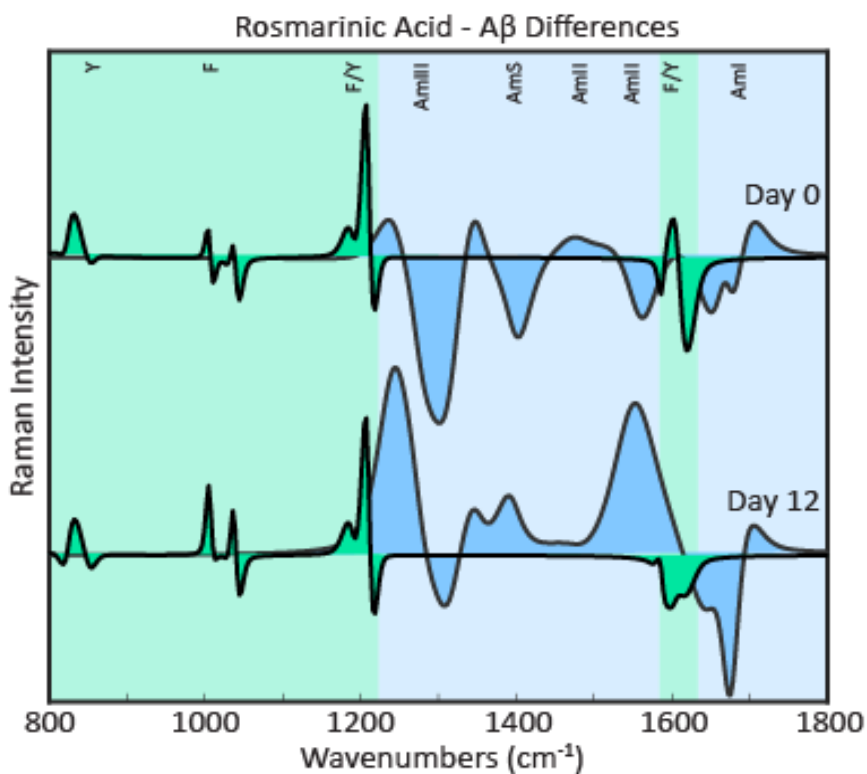
Figure 3.16: DUVRR difference spectra of the deconvoluted peaks of Aβ42 treated with rosmarinic acid and the untreated Aβ42 on Day 0 and Day 12. The amide modes are shown in blue and the aromatic modes are shown in green.

3.5 Discussion

As the polarity of the polyphenolic linker increased, the Aβ protein had a greater tendency to form a β-structure when exposed to polyphenols. Thus more non-polar linkers between the phenol rings should promote disordered structure. A more polar linker leads to the reduction of disordered content in Aβ and an increase in β-sheet structure. This was first observed by analyzing the CD spectra of Aβ with each polyphenol. Each polyphenol-treated Aβ samples starts off predominantly disordered protein structure on Day 0. The Day 0 CD spectra have the most intense minima at 197 nm, which was observed throughout the 12-day incubation period. The CD spectra of all the polyphenol-treated Aβ samples become less intense over time, but by differing amounts. The CD spectra indicate the nordihydroguaiaretic acid-treated Aβ changes structure only a very small amount and then the structure stabilizes. When curcumin was added to the sample, Aβ's structure remained disordered, but its structure slowly changed throughout the 12-day incubation period. Rosmarinic acid slowed but did not prevent formation of β-structure.

Previous studies have shown that when a protein goes from a disordered to β-sheet structure, changes in the dUVRR spectrum are minimal. There can be an overall loss of intensity, seen mainly in the amide modes, if aggregates form.[15] Also, a blue shift of the amide S mode in the dUVRR spectra can indicate β-sheet formation from disordered structure.[15] This shift is observed in dUVRR spectra of Aβ in the presence of polyphenols with linkers of increasing polarity (Figure 3.17). The Day 12 dUVRR spectra of Aβ with each polyphenol are stacked to show the peak shift. The

nordihydroguaiaretic acid-treated protein has the lowest peak maxima at 1394 cm^{-1}, followed by the curcumin-treated protein at 1397 cm^{-1}, and then the rosmarinic acid-treated protein, which occurs at 1405 cm^{-1}. The CD spectra of the rosmarinic acid-treated Aβ changed the most over time. Whereas the CD spectra of the nordihydroguaiaretic acid-treated Aβ remained stable, indicating the protein remained in a stable disordered structure over the 12-day incubation period. Thus, the dUVRR and CD data correlate well.
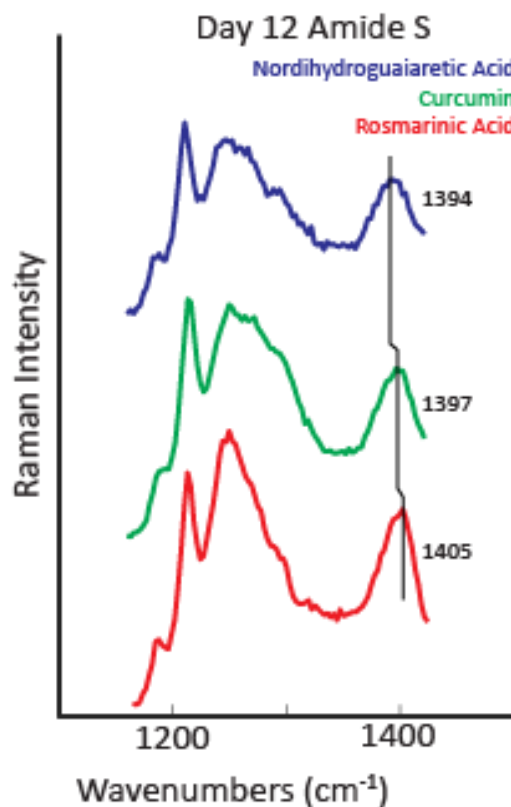
Figure 3.17: Blue shift of the amide S mode of Aβ; nordihydroguaiaretic acid (blue), curcumin (green), and rosmarinic acid (red) treatments.

DUVRR spectroscopy is useful for observing protein conformational changes, but the aromatic modes in dUVRR spectra are also useful for monitoring changes in the environment of aromatic residues within a protein. The two aromatic amino acids

present in Aβ are Y and F. For all polyphenol-treated Aβ samples, the Y mode at 820 cm^{-1} in dUVRR spectra decreased as compared to untreated Aβ samples. The Y mode at 858 cm^{-1} also decreases to the greatest extent with nordihydroguaiaretic acid treatment, whereas the Y mode at 1608 cm^{-1} decreases with all of the polyphenols tested. The more polar the chain linker, the more dramatic the observed decrease was observed. Another mode that follows this polarity trend is the F mode at 1008 cm^{-1}, for which only nordihydroguaiaretic acid, the least polar polyphenol, caused an increase in its intensity. Curcumin treatment caused a small decrease in this F mode, whereas and rosmarinic acid treatment caused a large decrease in the F mode intensity as compared to untreated Aβ. Among the polyphenols tested, the Y/F mode at 1213 cm^{-1} decreased the most dramatically when rosmarinic acid was added.

In general, the Y modes decreased in intensity over time when Aβ has been treated with polyphenolic compounds. Polyphenols containing a more polar chain linker, i.e., curcumin and rosmarinic acid, causes decreases in the F mode intensity, while a nonpolar chain linker as in nordihydroguaiaretic acid caused an increase in this mode. Increasing the polarity of the chain linker results in a greater change in the environment of the aromatic residues of the protein. This is seen in Figure 3.18, where Aβ samples treated with rosmarinic acid seem to have the largest differences in the aromatic regions.
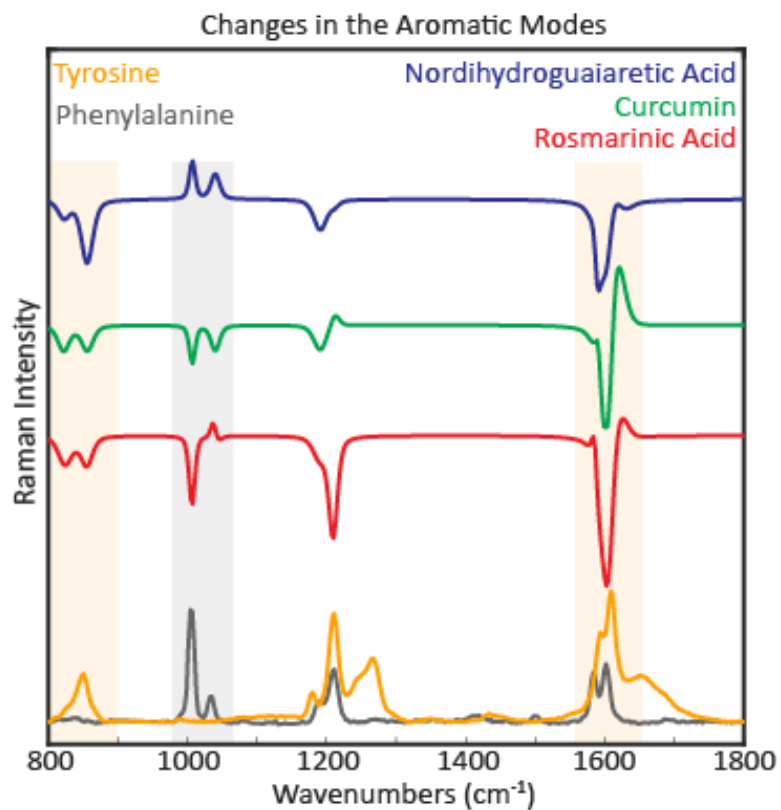
Figure 3.18: Changes over the 12-day incubation period in the individual aromatic modes of the dUVRR spectra. Nordihydroguaiaretic acid (blue), curcumin (green), and rosmarinic acid (red) are shown, as well as spectra of the aromatics tyrosine (orange) and phenylalanine (grey).

3.6 References

1. Lakey-Beitia, J.; Berrocal, R.; Rao, K. S.; Durant, A. A., Polyphenols as therapeutic molecules in Alzheimer's disease through modulating amyloid pathways. *Mol Neurobiol* **2015,** *51* (2), 466-479.

2. Ono, K.; Yoshiike, Y.; Takashima, A.; Hasegawa, K.; Naiki, H.; Yamada, M., Potent anti-amyloidogenic and fibril-destabilizing effects of polyphenols in vitro: implications for the prevention and therapeutics of Alzheimer's disease. *J Neurochem* **2003,** *87* (1), 172-181.

3. Shoval, H.; Lichtenberg, D.; Gazit, E., The molecular mechanisms of the anti-amyloid effects of phenols. *Amyloid* **2007,** *14* (1), 73-87.

4. Porat, Y.; Abramowitz, A.; Gazit, E., Inhibition of amyloid fibril formation by polyphenols: structural similarity and aromatic interactions as a common inhibition mechanism. *Chem Biol Drug Des* **2006,** *67* (1), 27-37.

5. Gazit, E., Mechanisms of amyloid fibril self-assembly and inhibition: Model short peptides as a key research tool. *FEBS J* **2005,** *272*, 5971-5978.

6. Gazit, E., Global analysis of tandem aromatic octapeptide repeats: The significance of the aromatic-glycine motif. *Bioinformatics* **2002,** *18* (6), 880-883.

7. Porat, Y.; Mazor, Y.; Efrat, S.; Gazit, E., Inhibition of islet amyloid polypeptide fibril formation: a potential role for heteroaromatic interactions. *Biochem* **2004,** *43*, 14454-14462.

8. Azriel, R.; Gazit, E., Analysis of the minimuml amyloid-forming fragment of the islet amyloid polypeptide. An experimental support for the key role of the phenylalanine residue in amyloid formation. *J Biol Chem* **2001,** *276* (36), 34156-24161.

9. Hudson, S. A.; Ecroyd, H.; Dehle, F. C.; Musgrave, I. F.; Carver, J. A., (-)-Epigallocatechin-3-gallate (EGCG) maintains kappa-casein in its pre-fibrillar state without redirecting its aggregation pathway. *J Mol Biol* **2009,** *392* (3), 689-700.

10. Convertino, M.; Pellarin, R.; Catto, M.; Carotti, A.; Caflisch, A., 9,10-Anthraquinone hinders beta-aggregation: how does a small molecule interfere with Abeta-peptide amyloid fibrillation? *Protein Sci* **2009,** *18* (4), 792-800.

11.	Lashuel, H. A.; Hartley, D. M.; Balakhaneh, D.; Aggarwal, A.; Teichberg, S.; Callaway, D. J., New class of inhibitors of amyloid-beta fibril formation. Implications for the mechanism of pathogenesis in Alzheimer's disease. *J Biol Chem* **2002,** *277* (45), 42881-42890.

12.	Arteaga, S.; Andrade-Cetto, A.; Cárdenas, R. Larrea tridentate (Creosote bush), an abundant plant of Mexican and US-American deserts and its metabolite nordihydroguaiaretic acid. *J Ethnopharmacol* **2005,** *98 (3),* 231–239.

13.	Gupta, S. C.; Kismali, G.; Aggarwal B. B. Curcumin, a component of turmeric: from farm to pharmacy. *Biofactors* **2013,** *39 (1),* 2-13.

14.	al-Sereiti, M. R.; Abu-Amer, K. M.; Sen, P. Pharmacology of rosemary (Rosmarinus officinalis Linn.) and its therapeutic potentials. *Indian J Exp Biol* **1999,** *37 (2),* 124-130.

15.	Oladepo, S. A.; Xiong, K.; Hong, Z.; Asher, S. A.; Handen, J.; Lednev, I. K. UV resonance Raman investigations of peptide and protein structure and dynamics. *Chem Rev* **2012**, 112, 2604-2628.

Chapter IV: Increasing Ring Substituents Destabilizes Pre-formed Amyloid-β Fibrils

4.1 Abstract

Stilbenoid compounds have common structural components consisting of two phenolic rings with hydroxyl group substituents and a chain linker between the rings. Hydroxyl groups on polyphenolic rings not only facilitate hydrogen bonding with the protein backbone, but also provide the compound with the ability to be an antioxidant. The antioxidant capacity increases with the number of hydroxyl substituents. This study investigated the ability of stilbenoid compounds differing in the number of hydroxyl substituents, to destabilize pre-formed Aβ fibrils. The polyphenols diethylstilbestrol, resveratrol, and piceatannol are structurally similar, but differ in the number of hydroxyl group substituents, i.e., two, three, and four, respectively. It was found that with increased number of hydroxyl ring substituents, pre-formed Aβ fibrils were destabilized more readily by the polyphenol.

4.2 Introduction

Hydroxyl group substituents on polyphenolic rings allow for essential binding to the protein through hydrogen bonds from the polyphenol to the amide rich backbone of the protein.[1-3] Studies have shown that the more hydroxyl groups, the higher the antioxidant activity.[4] Ono et al. compared four flavonoid compounds (myricetin, morin, quercetin, and kaempferol) that have similar structures and differ only in the numbers of hydroxyl substituents. It was found that decreasing the number of hydroxyl substituents decreased the anti-amyloidogenic and fibril-destabilizing activities of the polyphenol.[4] Polyphenols can act on Aβ aggregation at three different stages; initial formation of fibrils, extension of formed fibrils, and destabilization of pre-formed Aβ fibrils. A polyphenol may act at only one of these stages or possibly at all three.[4,5]

In Chapter 2, it was shown that increasing the number of hydroxyl substituents on polyphenols incubated with Aβ retarded structural changes that promote progression from a disordered to β-sheet structure. Using the same polyphenols as in Chapter 2 (i.e., diethylstilbestrol, resveratrol, and piceatannol), their effect on destabilization of pre-formed Aβ fibrils was assessed. The polyphenols diethylstilbestrol, resveratrol, and piceatannol shown in Figure 4.1 have an increasing numbers of hydroxyl substituents on their rings, having two, three, and four, respectively. They each have a 2-atom carbon chain between the two rings allowing for a conjugated double bond system. This study aims to examine how the number of hydroxyl group substituents affects the polyphenol's ability to destabilize pre-formed Aβ fibrils.
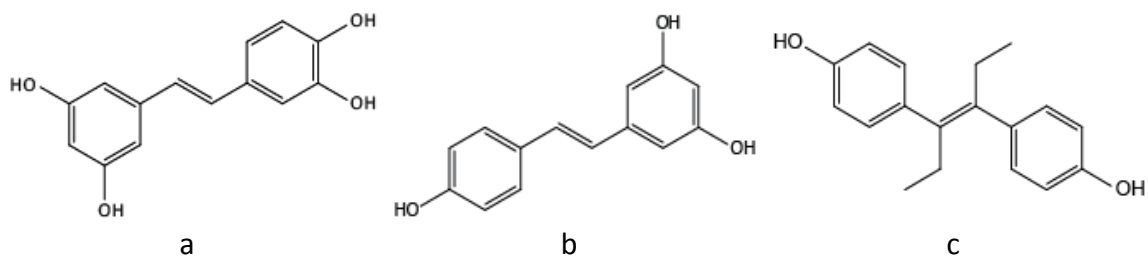
Figure 4.1: Structures of piceatannol (a), resveratrol (b), and diethylstilbestrol (c).

4.3 Materials and Methods

4.3.1 Materials

Aβ (1-42) (>95% pure) was purchased from Atlantic Peptides (Scarborough, ME). Ethanol and sodium perchlorate were purchased from Sigma-Aldrich (St. Louis, MO) and used without further purification. Sodium phosphate monobasic, sodium phosphate dibasic, sodium chloride, and cyclohexane were purchased from Fisher Scientific (Pittsburgh, PA). Thioflavin T, resveratrol, piceatannol, and diethylstilbestrol were purchased from Sigma-Aldrich (St. Louis, MO).

4.3.2 Amyloid- β (1-42) Protein Preparation

Aβ (1-42) (M.W. 4512.3 kDa) was dissolved in 10 mM sodium phosphate buffer, 20 mM NaCl, pH 7.4, sonicated for 10 min in an ice bath and centrifuged for 30 minutes at 14,000 rcf and 4°C (Centrifuge 5804 R, Eppendorf AG, Hamburg Germany). The concentration was estimated using the extinction coefficient of tyrosine, which is 1,280 $M^{-1}cm^{-1}$ at 280 nm using a Varian Cary Bio 50 UV-Vis spectrophotometer (Varian, Palo Alto, CA)[6]. Peptide concentrations ranged from 70-80 µM and were normalized in all the spectral processing. Aβ was prepared and incubated at 37°C for a 12-day time period. During this time, samples were characterized every two days by CD spectroscopy. Stock solutions of each polyphenolic compound were prepared in

ethanol at a concentration of 5 mM. Polyphenolic compounds were then added to the

protein solutions on Day 6, mid-way through the incubation period, for a final

concentration of 25 µM.

4.3.3 Circular Dichroism (CD)

A Jasco J-815 CD Spectropolarimeter (Jasco, Easton, MD) was used to collect CD

spectra in the range of 190-250 nm. A scan speed of 50 nm/min with a response time of

4 sec was used. Five spectra were averaged for each sample. A 1 mm optical path

length quartz cuvette (Hellman, Plainview, NY) was employed for all measurements.

4.3.4 Thioflavin T Assays

Fluorescence was measured on a Cary Eclipse spectrometer (Varian, Palo Alto,

CA). A 3 mm path length quartz cuvette (Hellman Plainview, NY) was employed for all

measurements. The emission spectra were measured using an excitation wavelength of

450 nm, and the fluorescence was collected from 470-700 nm.

4.3.5 Data Analysis

Data analysis was carried out in the MATLAB R206b (MathWorks, Natick, MA)

environment. For CD, all spectra were averaged and the background buffer spectrum

was subtracted from the raw data. The mean residue ellipticity (θ_{MRE}) was calculated

using Equation 1 with ϑ being the raw ellipticity from the measurement (degrees), *MW*

being the molecular weight of the protein (g/mol), *n* being the number of protein

residues, *d* being the path length of the cell (cm), and *C* being the concentration of the

sample (M).[6-8] All spectra were the average of triplicate trials.

Equation 1:

$$[\theta_{MRE}] = \frac{\theta \cdot MW}{10 \cdot n \cdot d \cdot C}$$

4.4 Results

4.4.1 Aβ Untreated

Aβ samples were prepared and incubated for 12 days. Figure 4.2 shows the CD spectra of Aβ incubated at 37°C over a 12-day period. On Day 0, the CD spectrum indicates that the protein is predominantly disordered. By Day 6, the protein was beginning to form β-sheet structure. The ThT assays indicated that the increase in β-sheet formation was associated with an increase in fibrils which is correlated with an increase in ThT fluorescence intensity (Figure 4.3). The CD spectra of Aβ on Days 8-12 indicate the complete loss of any disordered content. A single minimum present around 217 nm indicated that the peptide is predominantly β-sheet structured. There is a general loss in the overall intensity of the CD spectra in a manner that would suggest that the protein concentration may be decreasing over time. It is possible that more of the protein starts to form β-sheet structures, small oligomers form. These oligomers can be soluble or insoluble. The insoluble oligomers may fall out of solution causing the spectrum to lose intensity in all regions.
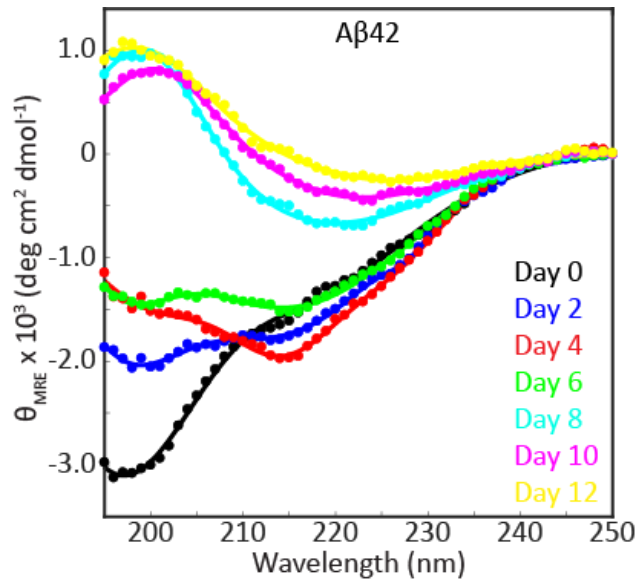
Figure 4.2: CD spectra of Aβ42 over a 12-day incubation period; Day 0 (black), Day 2 (blue), Day 4 (red), Day 6 (green), Day 8 (cyan), Day 10 (pink), and Day 12 (yellow).
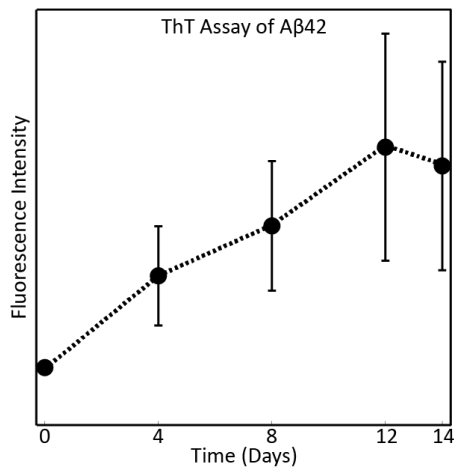
Figure 4.3: ThT fluorescence of Aβ42 fibrillization over a 14-day incubation period.

4.4.2 Piceatannol

Piceatannol, which has four hydroxyl substituents, shifted the structure of Aβ
from β-sheet to disordered which is evidenced by the re-emergence of a minima at 197
nm in the CD spectra (Figure 4.4). The CD spectra did not change dramatically over the
remaining 6 days, though the minima at 217 nm decreased in intensity slightly indicating
a small progressive loss in the remaining β-sheet content.
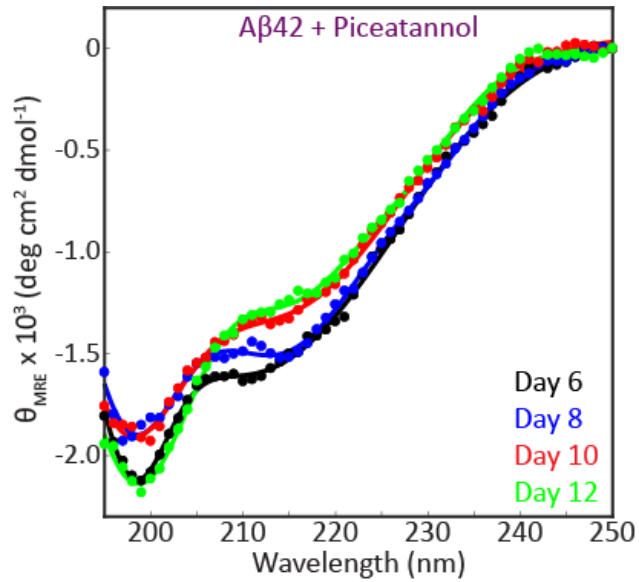
Figure 4.4: CD spectra of Aβ42 treated with piceatannol midway during a 12-day incubation period. The Aβ protein was treated with piceatannol on Day 6 (black). The protein continued to incubate through Day 8 (blue), Day 10 (red), and Day 12 (green).

4.4.3 Resveratrol

Resveratrol, which has three hydroxyl substituents, also shifted the structure of Aβ from β-sheet to disordered, based on the appearance of a minima at 197 nm in the CD spectrum (Figure 4.5). Although the addition of piceatannol and resveratrol had very similar immediate effects on Aβ's structure, the minima at 197 nm completely disappeared between Days 10 and 12 indicating the resveratrol did not prevent β-sheet formation after destabilizing fibrils. These data indicate that resveratrol can destabilize the β-sheet structure in the fibrils or protofibrils but is not able to prevent their re-formation. It is possible that oxidation of resveratrol makes it less effective at later points. In Chapter 2, it was observed the resveratrol delayed but did not prevent β-sheet formation, which is consistent with these results.
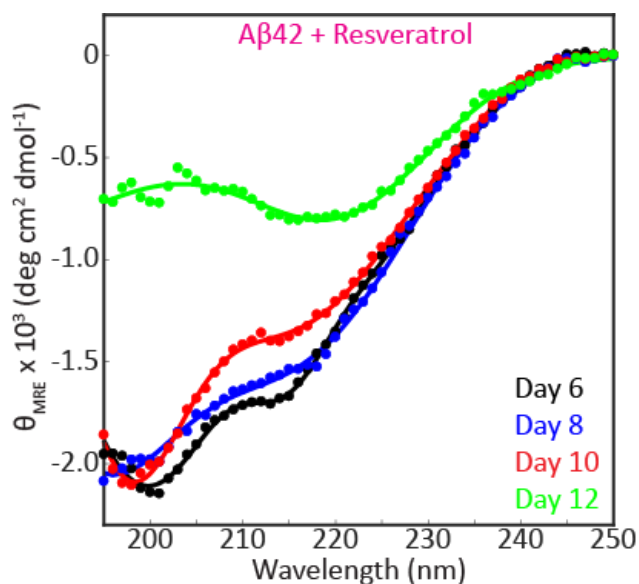
Figure 4.5: CD spectra of Aβ42 treated with resveratrol midway during a 12-day incubation period. The Aβ protein was treated with resveratrol on Day 6 (black). The protein continued to incubate through Day 8 (blue), Day 10 (red), and Day 12 (green).

4.4.4 Diethylstilbestrol

Diethylstilbestrol, which has two hydroxyl substituents, appears to promote β-sheet formation as evidenced by a stronger minima at 215 nm (Figure 4.6). On Day 6, with the addition of the polyphenol to the Aβ sample, a very small feature with a minimum at 197 nm is seen, however this feature is small in comparison to the other minimum at 215 nm. By Day 8, this feature is no longer present in the CD spectrum and the protein continues to stay predominantly β-sheet in structure. The overall loss in intensity of the spectra is similar to that of the untreated Aβ sample most likely due to the formation of insoluble small oligomers.
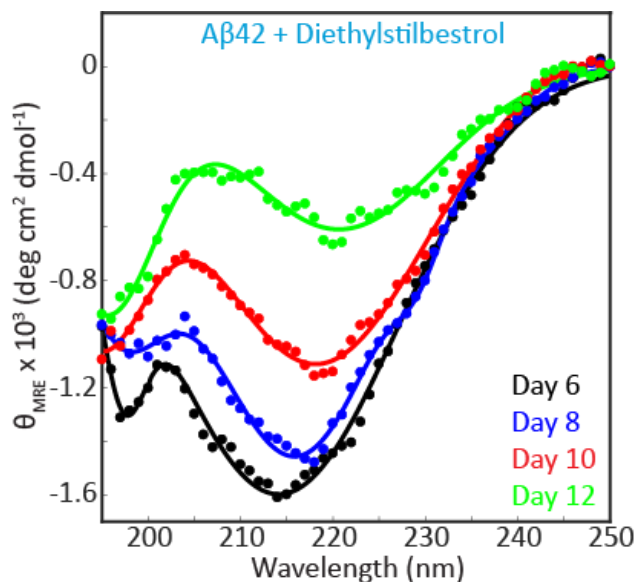
Figure 4.6: CD spectra of Aβ42 treated with diethylstilbestrol midway during a 12-day incubation period. The Aβ protein was treated with diethylstilbestrol on Day 6 (black). The protein continued to incubate through Day 8 (blue), Day 10 (red), and Day 12 (green).

4.5 Discussion

As the number of hydroxyl substituents is increased on the rings, the polyphenol is more capable of destabilizing the pre-formed Aβ fibrils. Piceatannol, with 4 hydroxyl groups, has an immediate effect on the secondary structure, changing the structure of

the Aβ protein from β-sheet to disordered. This effect remained throughout the incubation period. Resveratrol, with 3 hydroxyl groups, initially promoted disordered structure in the Aβ protein, however the polyphenol was incapable of preventing the protein from reforming fibrils potentially due to a loss of activity over time. Diethylstilbestrol, with only 2 hydroxyl groups, had a limited initial effect on the protein's structure. The protein formed predominantly β-sheet structure similar to the untreated Aβ solution.

Figure 4.7 shows the intensity of the CD spectra of untreated and treated samples at 217 nm. Evaluation of the intensity of the CD spectra at 217 nm, shows that the structure of the piceatannol-treated sample is relatively stable over time. The resveratrol-treated Aβ sample is also is fairly stable with changes in structure occurring after Day 10. The diethylstilbestrol-treated Aβ sample has the most noticeable change in structure when compared to the other two polyphenols. Diethylstilbestrol is the least effective polyphenol in destabilizing pre-formed Aβ fibrils. Thus, increasing the number of hydroxyl substituents, which increases the antioxidant potency of the polyphenol, makes the polyphenol capable of destabilizing pre-formed Aβ fibrils.
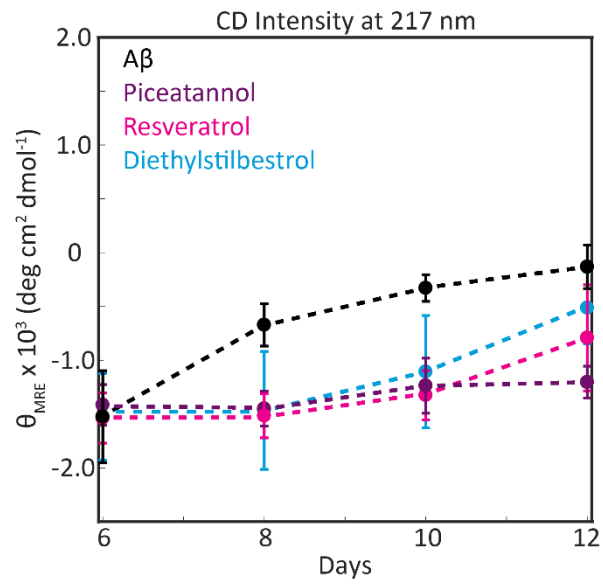
Figure 4.7: Intensity changes at 217 nm of the polyphenol-treated and untreated Aβ samples, over a 6-day incubation period; piceatannol (purple), resveratrol (pink), diethylstilbestrol (blue), and Aβ (black). Error bars are shown based on three repetitive trials.

4.6 References

1. Lakey-Beitia, J.; Berrocal, R.; Rao, K. S.; Durant, A. A., Polyphenols as therapeutic molecules in Alzheimer's disease through modulating amyloid pathways. *Mol Neurobiol* **2015,** *51* (2), 466-479.

2. Porat, Y.; Abramowitz, A.; Gazit, E., Inhibition of amyloid fibril formation by polyphenols: structural similarity and aromatic interactions as a common inhibition mechanism. *Chem Biol Drug Des* **2006,** *67* (1), 27-37.

3. Gauci, A. J. C., M.; Giese, A.; Scerri, C.; Vassallo, V. , Identification of polyphenolic compounds and black tea extract as potent inhibitors of lipid membrane destabilization by A beta(42) aggregates - ResearchGate. *J Alz Dis* **2011,** *24* (4), 767-779.

4. Ono, K.; Yoshiike, Y.; Takashima, A.; Hasegawa, K.; Naiki, H.; Yamada, M., Potent anti-amyloidogenic and fibril-destabilizing effects of polyphenols in vitro: implications for the prevention and therapeutics of Alzheimer's disease. *J Neurochem* **2003,** *87* (1), 172-181.

5. Shoval, H.; Lichtenberg, D.; Gazit, E., The molecular mechanisms of the anti-amyloid effects of phenols. *Amyloid* **2007,** *14* (1), 73-87.

6. Wang, M.; JiJi, R.D. Spectroscopic detection of β-sheet structure in nascent Aβ oligomers. *J Biophotonics* **2011**, *4*, 637-644.

7.   Simpson, J. V.; Balakrishnan, G.; JiJi, R. D. MCR-ALS analysis of two-way UV resonance Raman spectra to resolve discrete protein secondary structural motifes. *Analyst* **2009,** *134,* 138-147.

8. Wang, M.; JiJi, R. D. Resolution of localized small molecule-Aβ interactions by deep-ultraviolet resonance Raman spectroscopy. *Biophys Chem* **2011,** *158,* 96-103.

Chapter V: Increasing Chain Linker Polarity Destabilizes Pre-formed Amyloid-β Fibrils

5.1 Abstract

Diaryl polyphenolic compounds have common structural components consisting of two phenolic rings with hydroxyl group substituents and a chain linker between the rings. The chain between the two phenol rings can vary significantly both in length and atom makeup, altering the anti-amyloidgenic properties of the polyphenol. Flavonoid compounds do not contain a chain linker and understanding how the chain linker can affect the activity of linear polyphenols is imperative. The aromatic rings of polyphenols are important for their binding to proteins and their effects on protein aggregation. The type of linker between these rings is also important because it could also affect protein binding and aggregation. The polyphenols nordihydroguaiaretic acid, curcumin, and rosmarinic acid have increasing polarity, respectively, in the chain linker region between the phenolic rings. Each of these polyphenols has four ring substituents and 4 - 6 atoms in their chain linker. In this study, it was found that all the polyphenols disrupted and at least partially reversed fibrillization, though no clear trend with polarity of the linker region was observed.

5.2 Introduction

The chain between the two phenol rings can vary significantly both in length and atom makeup. These differences have an important impact on how the polyphenol metabolizes and behaves.[1-2] It is suggested that the optimum chain length between the rings should be 2-6 atoms long.[3] Studies have shown that diaryl polyphenols such as curcumin, are better than flavonoids at inhibiting the amyloidogenic activity of Aβ possibly due to the type of chain linker in between the aromatic rings.[1-2]

The aromatic rings are important for polyphenol binding to proteins and their effect on protein aggregation. Aromatic rings of polyphenols provide the necessary hydrophobic interactions with proteins that can interrupt endogenous hydrophobic interactions within the protein which promote aggregation.[3,4-9] The rings of polyphenols have the necessary planarity to bind to Aβ in the hydrophobic groove, interrupting the π stacking, and preventing aggregation by intercalating within the β-sheets.[1, 4,10-11] The chain linker polarity determines the polyphenol's overall polarity and its ability to disrupt the hydrophobic interactions necessary for protein aggregation.

The polyphenols nordihydroguaiaretic acid, curcumin, and rosmarinic acid have increasing polarity respectively in the chain linker region between their phenolic rings. Each of these polyphenols has four ring substituents and 4 - 6 atoms in their chain linker. In Chapter 3, the effect of polarity in the chain linker region on the structure of the Aβ protein during the aggregation process was evaluated. It was shown that decreasing the polarity of the chain linker increased the ability of the polyphenol to interfere with Aβ fibrillization. Using the same polyphenols, i.e., nordihydroguaiaretic

acid, curcumin, and rosmarinic acid, shown in Figure 5.1, it was evaluated whether these

molecules can also destabilize pre-formed Aβ fibrils.

a   b   c
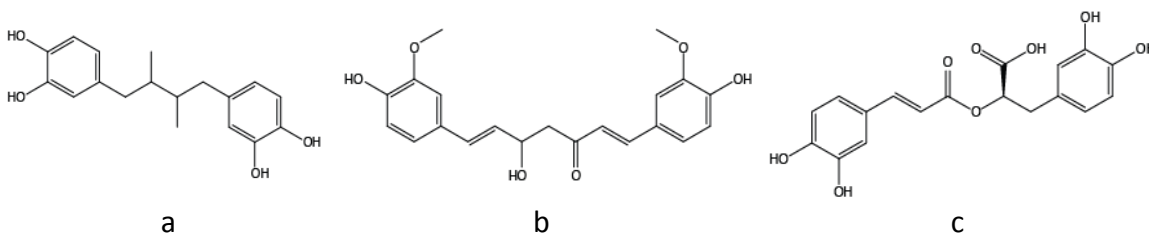
Figure 5.1: Structures of nordihydroguaiaretic acid (a), curcumin (b), and rosmarinic acid (c).

5.3   Materials and Methods

5.3.1   Materials

Aβ (1-42) (>95% pure) was purchased from Atlantic Peptides (Scarborough, ME).

Ethanol and sodium perchlorate were purchased from Sigma-Aldrich (St. Louis, MO) and

used without further purification. Sodium phosphate monobasic, sodium phosphate

dibasic, sodium chloride, and cyclohexane were purchased from Fisher Scientific

(Pittsburgh, PA). Thioflavin T, rosmarinic acid, and nordihydroguaiaretic acid were

purchased from Sigma-Aldrich (St. Louis, MO) and curcumin was purchased from Acros

Organics (Pittsburgh, PA).

5.3.2 Methods

The amyloid-β (1-42) protein was prepared and characterized as described in

Chapter 4, sections 4.3.2-4.3.4. Circular dichroism (CD) and were analyzed as described

in Chapter 4, section 4.3.5.

5.4 Results

5.4.1 Aβ Untreated

The initial CD spectra of the Aβ protein indicated that the protein was predominantly disordered in structure, with a strong minima at 197 nm (Figure 5.2). By Day 6, the protein had formed β-sheet fibrils as evidenced by the characteristic minima at 217 nm in the CD spectrum and concurrent increase in ThT fluorescence (Figure 5.3). Between Days 8-12 the CD spectra indicate a complete loss of any disordered content as the only minimum present is around 217 nm. The CD spectra generally lose overall intensity in a manner that would suggest that the protein concentration may be decreasing over time.
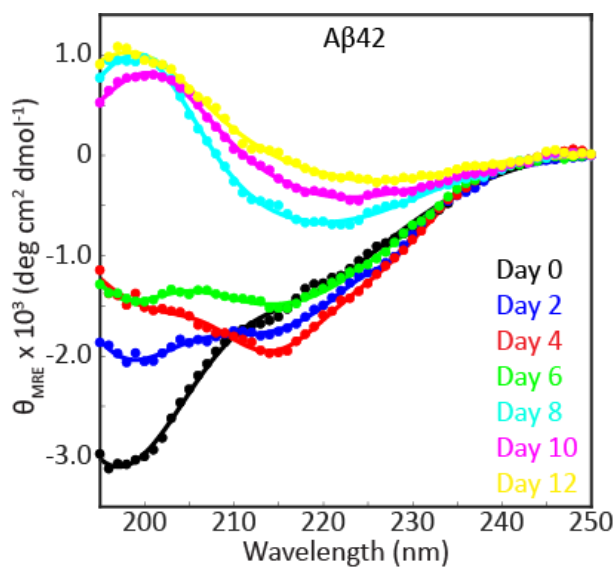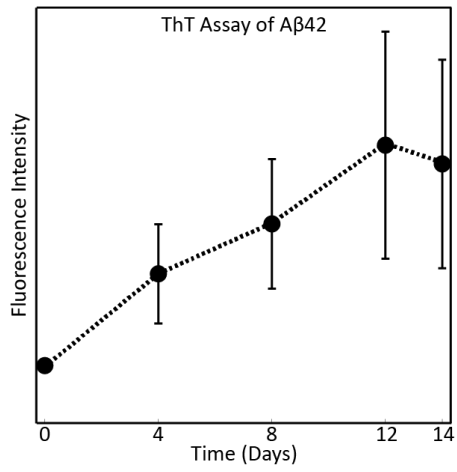

Figure 5.2: CD spectra of Aβ42 over a 12-day incubation period; Day 0 (black), Day 2 (blue), Day 4 (red), Day 6 (green), Day 8 (cyan), Day 10 (pink), and Day 12 (yellow).

Figure 5.3: ThT fluorescence of Aβ42 fibrillization over a 14-day incubation period.

5.4.2 Nordihydroguaiaretic Acid

Aβ was incubated at 37°C for 6 days. On Day 6, the polyphenols

nordihydroguaiaretic acid, curcumin, and rosmarinic acid were added to aliquots of the

Aβ protein solution. Nordihydroguaiaretic acid, having a nonpolar hydrocarbon chain

linker, was added to Aβ on Day 6 and the protein remained predominantly β-sheet

structured, as seen in Figure 5.4. However, a small disordered feature with a minimum

at 197 nm is seen, showing that there were initial structural perturbation by the

polyphenol on the protein. By Day 8, a loss in the intensity of the minima at 217 nm is

observed, which continues through Day 12. By Day 12, the protein is almost completely

disordered with appearance of the strong minimum at 197 nm and a significant loss of

the minimum at 217 nm. Although, the effects of nordihydroguaiaretic acid are slow,

the end result shows that the polyphenol does have the ability to destabilize pre-formed

Aβ fibrils.

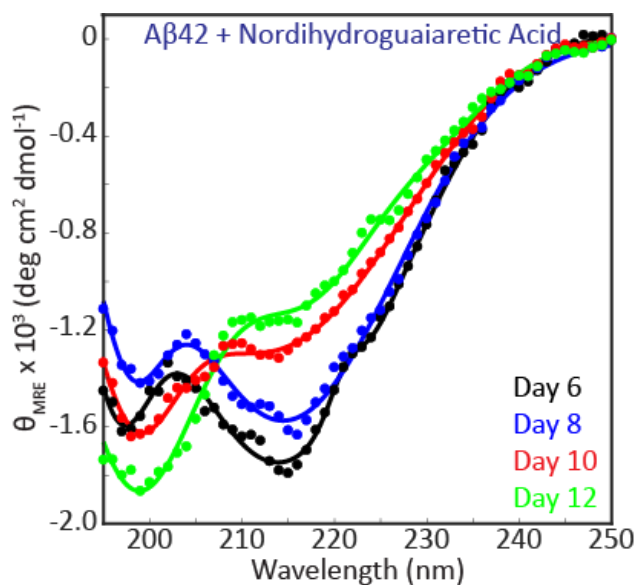*Figure 5.4: CD spectra of Aβ42 treated with nordihydroguaiaretic acid midway during a 12-day incubation period. The Aβ protein was treated with nordihydroguaiaretic acid on Day 6 (black). The protein continued to incubate through Day 8 (blue), Day 10 (red), and Day 12 (green).*

5.4.3 Curcumin

Curcumin, has a more polar chain linker than nordihydroguaiaretic acid. When curcumin was added to the Aβ sample on Day 6, the protein's structure stopped changing for the remainder of the incubation period. Additionally, curcumin immediately caused the protein to shift structure from predominantly β-sheet to partially disordered, as seen in Figure 5.5. Curcumin seems to stabilize the protein in an intermediate state with both disordered and β-sheet structures. With curcumin, the minimum at 197 nm indicative of disordered structure is more intense than the minimum at 217 nm which is indicative of β-sheet structure, showing that the destabilizing effects of curcumin are strong.

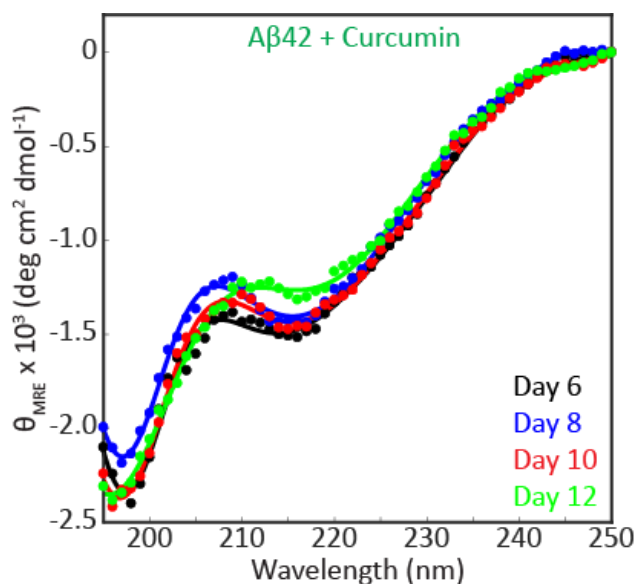*Figure 5.5: CD spectra of Aβ42 treated with curcumin midway during a 12-day incubation period. The Aβ protein was treated with curcumin on Day 6 (black). The protein continued to incubate through Day 8 (blue), Day 10 (red), and Day 12 (green).*

5.4.4 Rosmarinic Acid

Rosmarinic acid has the most polar chain linker. Again, it was added to the Aβ sample on Day 6. The structure of the protein immediately shifted toward a more disordered state with the minimum at 197 nm strengthening, as seen in Figure 5.6. There was still a slight feature at 217 nm suggestive of residual β-sheet structure, however the intensity of this feature reduces at each of the following time points.
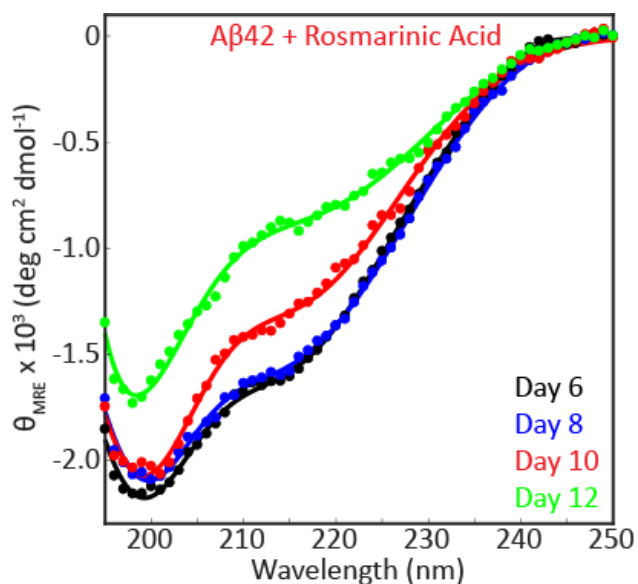
Figure 5.6: CD spectra of Aβ42 treated with rosmarinic acid midway during a 12-day incubation period. The Aβ protein was treated with rosmarinic acid on Day 6 (black). The protein continued to incubate through Day 8 (blue), Day 10 (red), and Day 12 (green).

5.5 Discussion

Each of the polyphenols tested here caused a shift from β-sheet to more disordered structure when added to pre-formed fibrils. However, the effect manifested differently for each polyphenol. Interestingly nordihydroguaiaretic acid appeared to initially promote β-sheet structure and then disrupt it over the remaining 6 days of incubation. Curcumin on the other hand, appeared to freeze Aβ in an intermediate state containing significant amounts of both disordered and β-sheet structures. Rosmarinic

acid also shifted the overall structure of Aβ toward disordered structure and continued

to do so throughout the experiment. Although there is no clear trend with the increase

in the polarity of the chain linker region, all three polyphenols disrupted the fibrillization

process. Nordihydroguaiaretic acid and rosmarinic acid continued to disrupt fibrils

throughout the remaining incubation period but curcumin appeared to freeze the

peptide in an intermediate state. Curcumin has the longest linker region between the

phenols, which may be a factor.

5.6 References

1.   Lakey-Beitia, J.; Berrocal, R.; Rao, K. S.; Durant, A. A., Polyphenols as therapeutic molecules in Alzheimer's disease through modulating amyloid pathways. *Mol Neurobiol* **2015,** *51* (2), 466-479.

2.   Ono, K.; Yoshiike, Y.; Takashima, A.; Hasegawa, K.; Naiki, H.; Yamada, M., Potent anti-amyloidogenic and fibril-destabilizing effects of polyphenols in vitro: implications for the prevention and therapeutics of Alzheimer's disease. *J Neurochem* **2003,** *87* (1), 172-181.

3.   Shoval, H.; Lichtenberg, D.; Gazit, E., The molecular mechanisms of the anti-amyloid effects of phenols. *Amyloid* **2007,** *14* (1), 73-87.

4.   Porat, Y.; Abramowitz, A.; Gazit, E., Inhibition of amyloid fibril formation by polyphenols: structural similarity and aromatic interactions as a common inhibition mechanism. *Chem Biol Drug Des* **2006,** *67* (1), 27-37.

5.   Gazit, E., Mechanisms of amyloid fibril self-assembly and inhibition: model short peptides as a key research tool. *FEBS J* **2005,** *272*, 5971-5978.

6.   Gazit, E., Global analysis of tandem aromatic octapeptide repeats: The significance of the aromatic-glycine motif. *Bioinformatics* **2002,** *18* (6), 880-883.

7.   Porat, Y.; Mazor, Y.; Efrat, S.; Gazit, E., Inhibition of islet amyloid polypeptide fibril formation: a potential role for heteroaromatic interactions. *Biochem* **2004,** *43*, 14454-14462.

8.   Azriel, R.; Gazit, E., Analysis of the minimuml amyloid-forming fragment of the islet amyloid polypeptide. An experimental support for the key role of the phenylalanine residue in amyloid formation. *J Biol Chem* **2001,** *276* (36), 34156-61.

9.   Hudson, S. A.; Ecroyd, H.; Dehle, F. C.; Musgrave, I. F.; Carver, J. A., (-)-Epigallocatechin-3-gallate (EGCG) maintains kappa-casein in its pre-fibrillar state without redirecting its aggregation pathway. *J Mol Biol* **2009,** *392* (3), 689-700.

10.   Convertino, M.; Pellarin, R.; Catto, M.; Carotti, A.; Caflisch, A., 9,10-Anthraquinone hinders beta-aggregation: how does a small molecule interfere with Abeta-peptide amyloid fibrillation? *Protein Sci* **2009,** *18* (4), 792-800.

11.   Lashuel, H. A.; Hartley, D. M.; Balakhaneh, D.; Aggarwal, A.; Teichberg, S.; Callaway, D. J., New

class of inhibitors of amyloid-beta fibril formation. Implications for the mechanism of

pathogenesis in Alzheimer's disease. *J Biol Chem* **2002,** *277* (45), 42881-90.

Chapter VI: Conclusions

The aggregation pathway of the amyloid-β protein can be altered by introduction of polyphenolic compounds. This alteration can occur during the formation and extension stages of the aggregation, or during the destabilization stage of the pathway. How a polyphenol behaves when introduced to the protein solution is dependent both on chain linker polarity and number of hydroxyl ring substituents on the polyphenol. This investigation examined the effects of nordihydroguaiaretic acid, curcumin, rosmarinic acid, resveratrol, piceatannol, and diethylstilbestrol on Aβ aggregation and destabilization using circular dichroism and deep ultraviolet resonance Raman spectroscopies.

Increasing the number of ring substitutions was correlated with an increased ability to prevent of the formation of fibrils and also to destabilize pre-formed fibrils. Increasing the hydroxyl group substituents on the polyphenol likely facilitates increased hydrogen bonding required with Aβ. The polyphenols diethylstilbestrol, resveratrol, and piceatannol have increasing numbers of hydroxyl substituents on their rings, having two, three, and four respectively. Piceatannol, having the greatest number of hydroxyl substituents has the highest efficacy in preventing formation of fibrils and destabilizing pre-formed fibrils.

Increasing the polarity of the chain linker resulted in decreased stability of the protein during the aggregation process. The nonpolar chain linker of nordihydroguaiaretic acid preserved the disordered structure of the Aβ protein and prevented it from forming β-sheet structure. Conversely, rosmarinic acid having the

most polar chain linker was not able to perform in the same manner, increasing the amount of β-sheet structure in the protein solution. Nordihydroguaiaretic acid, curcumin, and rosmarinic acid were able to disrupt pre-formed Aβ fibrils, each at its own rate, however the final state was similar regardless of added polyphenol. Decreasing the polarity of the chain linker would be optimal in order to prevent, or slow, the formation of fibrils while still having the ability to destabilize pre-formed Aβ fibrils as well.

Future studies including a wider array of polyphenols with varying phenolic ring substitutions and chain linkers is necessary to confirm the results shown here. Amyloid-β has many unique fragments within its 42 residues which all play a different role in how the protein aggregates. Examples of these fragments include the transmembrane region, extracellular region, glycine zipper motifs, HHQK motif, and KLVFF motif. Investigating how the different structural components of the polyphenols affect each of these Aβ fragments is crucial to gain a full understanding on how they are playing a role in the complete aggregation pathway of Aβ.

VITA

Brittany L. Hagenhoff was born on August 2nd, 1990 in Jefferson City, Missouri where she was raised. She attended the University of Central Missouri where she obtained her B.S. in Chemistry in the Spring of 2012. She received a Ph. D. in Chemistry under the supervision of Dr. Renee D. JiJi at the University of Missouri-Columbia, with a graduation date of Fall 2017. She attained a position as a tenure track analytical faculty member at Truman State University in Kirksville, Missouri beginning in the Fall of 2017.